Performance of a Lean-Burn Natural Gas Engine using a Double-Pulse Partially-Stratified Charge Ignition System

by

Arminta S Chicka

B.ASc., The University of British Columbia, 2009

A THESIS SUBMITTED IN PARTIAL FULFILMENT OF
THE REQUIREMENTS FOR THE DEGREE OF

Masters of Applied Science

in

The Faculty of Graduate Studies

(Mechanical Engineering)

The University Of British Columbia

(Vancouver)

April 2012

Abstract

Natural gas is one of the cleanest burning hydrocarbon fuels due to it being mostly methane. Methane has the highest carbon to hydrogen ratio and therefore has the lowest CO_2 emissions per unit of energy produced when burned. This combined with the abundance of natural gas reserves worldwide, makes it an appealing alternative fuel. While natural gas is a cleaner burning fuel than gasoline or diesel, there are still harmful emissions that result from it's combustion. In order to reduce these emissions, lean burn engines are being employed.

A lean burn engine runs using an air-fuel ratio that has excess air compared to the stoichiometic air-fuel ratio. When the amount of excess air is significant, the engine runs cooler and produces less nitrogen oxides (NO_X). This is important since NO_X emissions contribute to smog which effects human health and the environment. Another benefit of lean burn engines it that, for those using a homogeneous charge, the leaner the engine can run, the wider the load range available without having to throttle the air-fuel mixture. Throttling is undesirable because it causes energy losses by restricting the flow of the air-fuel mixture being drawn into the engine.

To extend the load range over which a natural gas lean-burn spark-ignited engine can operate, a method that uses a partially-stratified charge (PSC) has been proven to be useful. The PSC is produced by injecting a small amount of fuel (less than 5% of the

total fuel mass) directly into the engine combustion chamber near the spark plug. This creates a comparatively rich air-fuel ratio near the spark plug which is easily ignited creating a strong flame front that moves through the rest of the homogenous lean air-fuel mixture. To extend the load range even further, a method of PSC that uses two direct injections, one before spark and one after, has been tested and is described in this thesis.

The most effective single-pulse injection (SPI) conditions (pressure, injection size and timing) were used for the injection occurring before the spark then a secondary injection was added after the spark using the same injection pressure. The results showed no improvement in engine performance using the double-pulse injection (DPI) method over the SPI method. Engine performance was similar for the SPI case and the DPI cases where the secondary injection was small and there was a decrease in engine performance for the DPI cases with larger secondary injections.

Although no improvement in overall engine performance was seen using the DPI method employed, there were improvements in IMEP for engine cycles where ignition was successful. If the best primary and secondary-injection conditions could be determined, there would likely be improvements in overall engine performance compared to the single-injection case. More testing is required to determine whether the DPI method can be successful at improving overall engine performance.

Table of Contents

Abstract ii

Table of Contents iv

List of Tables vi

List of Figures vii

Nomenclature ix

Acknowledgements xii

Dedication xiii

1 Introduction 1
1.1 Previous Research 2
1.2 Research Objectives 10

2 Experimental Set-up 12
2.1 PSC Set-up 12
2.2 Engine 15
2.3 Data Acquisition Systems (DAQ) 16

3 Experimental Results and Discussion 17
3.1 Methodology 17
3.2 Preliminary Single-Injection-PSC Optimization Tests 18
3.3 Main Double-Injection-PSC Tests 25
3.4 High λ Double-Injection Tests 55

4 Uncertainty Analysis 71

5 Conclusions and Recommendations 75
5.1 Conclusions 75
5.2 Recommendations 77

Bibliography 79

Appendix A Detailed Experimental Set-up 82
A.1 PSC Mechanical System 82
A.2 PSC Electrical System 84
A.3 PSC System Timing Characteristics 94
A.4 Fuel 94

Appendix B Calculated Values 96
B.1 Relative Air-Fuel Ratio (λ) 96
B.2 Brake Specific Fuel Consumption (BSFC) 96
B.3 Coefficient of Variation of Indicated Mean Effective Pressure (COV of IMEP) 97
B.4 Thermal Efficiency 98
B.5 Brake Specific Methane ($BSCH_4$) 98

B.6 Brake Specific Nitrogen Oxides(BSNOx) 99

Appendix C Detailed Uncertainty Analysis 100
C.1 Engine and Emissions Instrumentation Uncertainties 100
C.2 Root-Sum-Squared Uncertainty Calculations 102
C.3 Example Uncertainty Calculation 102

Appendix D Standard Engine Operating Procedure 108

Appendix E Minimum Advance for Best Torque Technique 115

List of Tables

2.1 Engine Specifications 15
2.2 Spark Plug Specifications 15

3.1 Optimum Engine Performance Parameters for Single-Injection-PSC . 25
3.2 PSC Flow Rates at 1500 rpm 26
3.3 PSC Flow Rates at 3000 rpm 39
3.4 PSC Flow Rates at 1500 rpm, $\lambda \geq 1.70$ 56

4.1 Test Descriptions 72
4.2 Calculated Uncertainties of λ and BSFC 72
4.3 Calculated Uncertainties of Brake Specific Emissions 73

A.1 Direct Injector Manufacturer's Specifications 83
A.2 Westport Natural Gas Composition Oct 3rd 2011 95

C.1 Engine and Emissions Instrumentation Specifications 101

List of Figures

1.1 Modified Spark Plug for PSC[5] 4

2.1 PSC Spark Plug Insert[10] 13

3.1 First Stage Preliminary Tests BSFC: 1500 rpm, λ = 1.55, 8 bar 21
3.2 First Stage Preliminary Tests COV of IMEP: 1500 rpm, λ = 1.55, 8 bar 22
3.3 Second Stage Preliminary Tests BSFC: 1500 rpm, λ = 1.65 23
3.4 Second Stage Preliminary Tests COV of IMEP: 1500 rpm, λ = 1.65 . 24
3.5 Injection Timing Diagram:λ= 1.75, 1500 rpm 27
3.6 DPI - BSFC vs.λ= 1.3-1.85 at 1500 rpm 28
3.7 DPI - BSFC vs.λ= 1.55-1.85 at 1500 rpm 29
3.8 DPI - COV of IMEP vs.λ= 1.55-1.85 at 1500 rpm 30
3.9 DPI - Thermal Efficiency vs.λ= 1.55-1.85 at 1500 rpm 31
3.10 IMEP vs CA of Maximum Pressure for No-PSC: 1500 rpm, λ = 1.65 . 32
3.11 IMEP vs CA of Maximum Pressure for SPI: 1500 rpm, λ = 1.65 . . . 33
3.12 Integrated Heat Release vs. Crank Angle: 1500 rpm, λ = 1.65 34
3.13 IMEP vs CA of Maximum Pressure for DPI 3ms Pulse Starting 2ms After Spark: 1500 rpm, λ = 1.75 35
3.14 DPI - $BSCH_4$ vs.λ= 1.55-1.85 at 1500 rpm 36
3.15 DPI - $BSNO_X$ vs.λ= 1.55-1.85 at 1500 rpm 37
3.16 Injection Timing Diagram:λ= 1.70, 3000 rpm 40
3.17 DPI - BSFC vs.λ= 1.55-1.75 at 3000 rpm 41
3.18 DPI - COV of IMEP vs.λ= 1.55-1.75 at 3000 rpm 42
3.19 DPI - Thermal Efficiency vs.λ= 1.55-1.75 at 3000 rpm 44
3.20 IMEP vs CA of Maximum Pressure for No-PSC: 3000 rpm, λ = 1.65 . 45
3.21 IMEP vs CA of Maximum Pressure for SPI: 3000 rpm, λ = 1.65 . . . 46
3.22 Integrated Heat Release vs. Crank Angle: 3000 rpm, λ = 1.65 47
3.23 IMEP vs CA of Maximum Pressure for SPI: 3000 rpm, λ = 1.75 . . . 48
3.24 IMEP vs CA of Maximum Pressure for DPI 1ms Pulse Starting 1ms After Spark: 3000 rpm, λ = 1.75 49
3.25 IMEP vs CA of Maximum Pressure for DPI 2ms Pulse Starting 0ms After Spark: 3000 rpm, λ = 1.75 50
3.26 Integrated Heat Release vs. Crank Angle: 3000 rpm, λ = 1.75 51
3.27 DPI - $BSCH_4$ vs.λ= 1.55-1.75 at 3000 rpm 52
3.28 DPI - $BSNO_X$ vs.λ= 1.55-1.75 at 3000 rpm 53
3.29 DPI - BSFC vs.λ= 1.70-1.85 at 1500 rpm 57
3.30 DPI - COV of IMEP vs.λ= 1.70-1.85 at 1500 rpm 58

3.31 DPI - Thermal Efficiency vs.λ= 1.70-1.85 at 1500 rpm 59
3.32 IMEP vs CA of Maximum Pressure for Low Flow SPI: 1500 rpm, λ = 1.80 60
3.33 IMEP vs CA of Maximum Pressure for High Flow SPI: 1500 rpm, λ = 1.80 61
3.34 IMEP vs CA of Maximum Pressure for DPI 1ms Pulse Starting 2ms After Spark: 1500 rpm, λ = 1.80 62
3.35 Integrated Heat Release vs. Crank Angle: 1500 rpm, λ = 1.80 63
3.36 IMEP vs CA of Maximum Pressure for High Flow SPI: 1500 rpm, λ = 1.85 64
3.37 IMEP vs CA of Maximum Pressure for DPI 1ms Pulse Starting 2ms After Spark: 1500 rpm, λ = 1.85 65
3.38 Integrated Heat Release vs. Crank Angle: 1500 rpm, λ = 1.85 66
3.39 DPI - BSCH_4 vs.λ= 1.70-1.85 at 1500 rpm 67
3.40 DPI - BSNO_X vs.λ= 1.70-1.85 at 1500 rpm 68

A.1 Siemens Gasoline Piezo Electric Direct Injector 83

E.1 MBT Spark Timing Graph 116

Nomenclature

Symbols

$\dot{m}_{air,dry}$	Mass Flow Rate of Dry Air
$\dot{m}_{fuel,homo}$	Mass Flow Rate of Fuel for Homogeneous Charge
$\dot{m}_{fuel,strat}$	Mass Flow Rate of Fuel for Stratified (PSC) Charge
$\dot{m}_{fuel}$	Mass Flow Rate of Fuel
$\dot{V}_{air}$	Volumetric Flow Rate of Air
λ	Relative Air-Fuel Ratio
$(A/F)_{stioch}$	Stiociometric Air-Fuel Ratio
μ_{std}	Standard Viscosity of Air
ω	Specific Humidity
ρ_{air}	Density of Air
$\triangle P_{LFE}$	Differential Pressure across the Laminar Flow Element
B	B Constant specific to LFE device
C	C Constant specific to LFE device
N	Engine Speed in rpm
P_{air}	Pressure of Intake Air
P_{H_2O}	Partial Pressure of Water Vapour
P_{sat,H_2O}	Staturation Pressure of Water in Intake Air
R_{air}	Gas Constant of Air
R_{H_2O}	Gas Constant for Water
T_{air}	Temperature of Intake Air
u	Uncertainty

Abbreviations

ABDC	After Bottom Dead Center
ATDC	After Top Dead Center
BBDC	Before Bottom Dead Center
BMEP	Brake Mean Effective Pressure
$BSCH_4$	Brake Specific Mathane
BSFC	Brake Specific Fuel Consumption
$BSNO_X$	Brake Specific Nitrogen Oxide
BStHC	Brake Specific total HydroCarbons
BTDC	Before Top Dead Center
CH_4	Methane
CO_2	Carbon Dioxide
COV	Coefficient of Variation
DC	Direct Current
DPI	Double Pulse Injection
FS	Full Scale
H_2O	Hydrogen Dioxide (Water)
IMEP	Indicated Mean Effective Pressure
LFE	Laminar Flow Element
NO_X	Nitrogen Oxide
O_2	Dioxide (Elemental Oxygen)
PSC	Partially Stratified Charge
RH	Relative Humidity
SPI	Single Pulse Injection
tHC	Total Hydrocarbons

Units

A	Amps
cc	Cubic Centimeters
g/kWhr	Grams per Kilowatt Hour

g/s	Grams per Second
kHz	Kilohertz
mg/stroke	Milligrams per Stroke
mH	Microhenry
MHz	Megahertz
mm	Millimeter
ms	Milliseconds
Nm	Newton Meter
ppm	Parts per Million
psi	Pounds per Square Inch
psig	Pounds per Square Inch Gauge
rpm	Revolutions per Minute
slm	Standard Litres per Minute
V	Volts
VDC	Volts Direct Current
º	Degree
ºC	Degrees Celcius
ºCA	Crank Angle Degrees

Acknowledgements

I would like to thank my supervisor, Professor Robert L. Evans, for his guidance with regards to this thesis. He offered an educational environment that was nurturing and also allowed for independent inquiry. I'd also like to thank Professor Steve Rogak and Dr. Philip Hill for assisting in troubleshooting problems with regards to improper engine operation. Bob Perry was another very helpful person who I would like to thank for his efforts with engine maintenance and repair. Without his assistance I would have wasted many days trying to figuring out engine repairs, not to mention the time he saved me by retrieving part of the PSC insert without pulling apart the engine.

I owe many thanks to Glenn Jolly for working tirelessly on the injector driver and going above expectations by writing a description of the electrical engine control system. I would also like to thank Dr. Ning Wu for helping me understand the emissions measurement system used in the lab and providing me with the natural gas composition used in this paper. Many thanks also goes to all my fellow graduate students, past and present, who aided me with my course and thesis work. Those students are: Edward Chan, Eshan Faghani, Malcolm Shield, Mahdi Salehi, Jean Logan, Eric Kastanis, Conor Reynolds and Bronson Patychuk.

Dedication

I would like to thank my boyfriend, Michael Maxwell, for supporting me through my long educational experience. He was 100% behind all my educational decisions and I thank him for that. I would also like to thank my son, Tré Rodgers, for his support and putting up with my extended work hours so I could complete my degree. I would like to thank my parents, Laila and Dennis Chicka, for their support, both emotional and financial, without which I would have not been able to undertake this degree.

Chapter 1

Introduction

In the world today, most of the energy consumed comes from burning oil products. However, there is concern over the environmental impacts this has as well as potential supply problems. Many other forms of energy are being considered as partial replacements, including alternatives fuels such as natural gas. Natural gas, which is 70-90% methane[2], has grown in popularity over the years due to its lesser environmental impact. The main advantage of methane is that compared to other hydrocarbon (fossil) fuels it produces the least amount of carbon dioxide (CO_2) per unit of energy when burned[3]. This means less greenhouse gases are emitted. Another factor that makes natural gas appealing is its abundance; there are 190 trillion cubic meters, or the equivalent to 1.2 trillion barrels of oil, of proven global natural gas reserves[1].

Addressing the issue of CO_2 emissions is not enough. The burning of fossil fuels produces other hazardous gases such as nitrogen oxides (NO_X) which leads to smog and ground level ozone[3]. Both of these negatively affect the health of humans, animals and plants. One of the most common means of reducing NO_X emissions from fossil fuel burning engines is to run the engine at a lean air-fuel ratio (λ). A lean air-fuel ratio means the engine is run with excess air compared to what is chemically required for complete combustion. The lean operation of these engines results in lower combustion temperatures which reduces the amount of NO_X produced[4].

Another advantage of lean engine operation is that throttling can be reduced thereby reducing the resulting pumping losses. By running the engine over a large range of air-fuel ratios to get the desired power output, the need to throttle the engine is reduced or even eliminated. The overall effect is lower fuel consumption for low load conditions.

1.1 Previous Research

There are three types of charges used for spark-ignited engines. The most common is the homogeneous charge where the fuel and air are mixed before entering the combustion chamber giving a homogeneous air-fuel mixture throughout the chamber. In recent years the stratified charge has become more popular due to it being more fuel efficient than the homogeneous charge. A stratified charge is the result of the fuel being injected directly into the combustion chamber giving a variation in air-fuel ratios throughout the combustion chamber. A partially stratified charge (PSC), which is used for the experiments in this thesis, is a combination of both a homogeneous and stratified charge.

1.1.1 Partially Stratified Charge Concept

Lean-burn engines offer some advantages over stoichiometric-burn engines with respect to emissions and throttling. As mentioned earlier, lean-burn engines have lower NO_X emissions and can avoid throttling losses by allowing the engine to operate over a large range of air-fuel ratios to achieve various loads instead of by use of a throttle. A major issue with running an engine lean is that as the air-fuel ratio becomes leaner

it becomes harder to ignite and combustion becomes variable. To improve ignition of the lean-homogeneous mixture a richer stratified charge has been added.

The objective is to use a small amount of fuel injected at the spark plug just before ignition to create a richer air-fuel ratio at the spark plug which is more easily ignited than the bulk lean air-fuel mixture. Once ignited the flame created can more readily ignite the bulk lean mixture than a spark could, due to its larger surface area. The method of supplying fuel at the spark plug to improve combustion was conceived and patented by Dr. Robert L. Evans in 2000[6].

The mass of the fuel injected at the spark plug is typically > 5% of the total fuel mass. Ideally, the relative air-fuel ratio (λ) of the the plume created due to the PSC injection would be around 1.0 so that it would be easily ignited by the spark. To look at this in terms of volume, consider the case where the overall λ= 1.80 with 5% of the fuel being injected at the spark plug. In this case the volume of the PSC plume would 2.8% the volume of the combustion chamber at the time of spark and the bulk charge would have a λ= 1.84.

The first method of providing a partial-stratified charge was by using a modified spark plug design. Fuel is supplied to the spark plug via a capillary tube, traveling through passages cut out in the spark plug and exits near the spark plug electrode. The fuel supplied is controlled using a solenoid valve and the fuel pressure is controlled using a regulator valve.

The modified spark plug was designed by Conor Reynolds and was tested using a single-PSC-injection timed to finish before spark. The test results were presented in

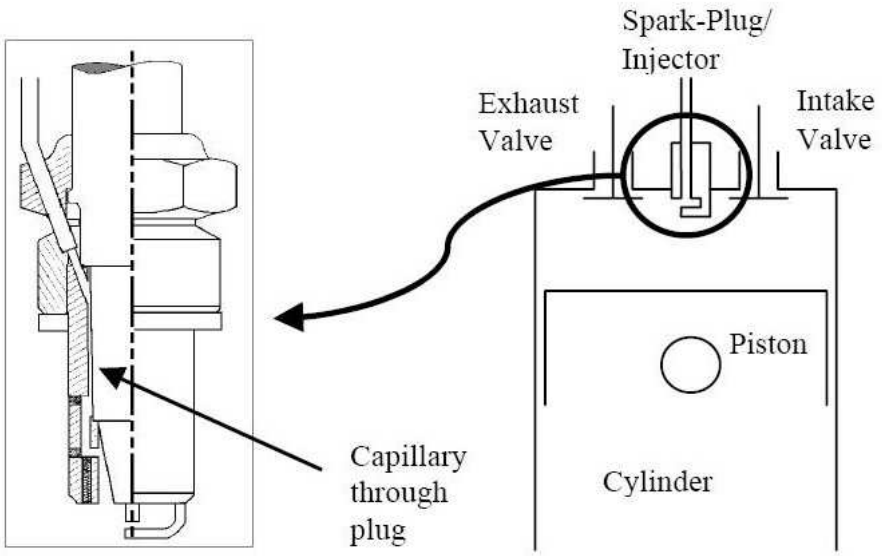

Figure 1.1: Modified Spark Plug for PSC[5]

his Masters thesis[5] as well as in papers by Evans[7, 8, 17]. The results of these tests showed that using a PSC injection of less than 5% of the total fuel mass significantly improved engine efficiency and power for λ greater than 1.5 at engine speeds of 2000 rpm and 2500 rpm but not at 1500 rpm. At 3000 rpm, it was not possible to inject enough fuel through the modified spark plug to improve engine efficiency or power. There was, however, improvements in carbon monoxide and total hydrocarbon emissions near the lean limit of combustion, the point where the coefficient of variation of gross indicated mean effective pressure (COV of IMEP) rises above 10%. Reynolds theorized that this was due to a small improvement in combustion from the use of the PSC injection and that if more fuel could be injected during the PSC injection, there would be improvements in engine efficiency and power at 3000 rpm, not just at 2000

rpm and 2500 rpm.

The following was pulled directly from the conclusions section of Reynolds Masters thesis [5] and further summarizes the results of previous research using PSC (Note: The "current" PSC system described here is referred to as the "old" or "previous" PSC system everywhere else in this thesis):

1. With the current Partially Stratified-Charge system, the lean misfire limit for the Ricardo Hydra engine was extended by approximately 5% at speeds of 2000rpm and 2500rpm. At all speeds tested, application of PSC at lean air-fuel ratios resulted in retardation of MBT spark timing.

2. Use of PSC at 2000rpm and 2500rpm resulted in a reduction of approximately 8% in brake specific fuel consumption at a relative air-fuel ratio of 1.65, and there was a corresponding increase in thermal efficiency. Engine power was increased by up to 7%.

3. At these speeds significant reductions in carbon monoxide and total hydrocarbon emissions were observed. Oxides of nitrogen increased slightly due to the increase in maximum cylinder pressure with PSC, but were found to be very low near the LML when compared with stoichiometric fueling.

4. A general improvement in combustion quality and stability occurred with PSC at lean air-fuel ratios at 2500rpm. The coefficient of variation of indicated mean effective pressure was reduced, maximum cylinder pressure increased and the overall combustion duration, from spark to 95% MFB, was reduced by up to 15% due to the implementation of PSC.

*End of reference to Reynolds Masters thesis. MBT refers to the minimum spark advance (timing before the engine piston reaches top dead center) that is required to achieve the best engine torque without producing knock, and is more thoroughly defined in Section E. LML is the Lean Misfire Limit or lean limit of combustion as described earlier in this section. MBF is the Mass Fraction Burned of the fuel that is combusted during one engine cycle.

1.1.2 Spark Plug Insert and Varying Injection Patterns

Using a modified spark plug meant that every time the spark plug needed to be replaced a new spark plug needed to be modified which was deemed to be too time consuming and costly. To resolve this issue, a spark plug insert was designed and manufactured. The insert threads into the spark plug hole in the engine head and contains the passageways that the modified spark plug did. A smaller spark plug than previously used is threaded into the insert and fuel is delivered from the insert to the spark plug electrode.

Improvements to the spark plug insert were made by Jean Logan by changing the injection pattern of the PSC fuel[10]. Previous designs of the modified spark plug and spark plug insert used a single hole to inject fuel toward the spark plug electrode. Since the injection pattern used for direct-injected stratified-charge engines can have a significant effect on combustion, it was theorized that by changing the injection pattern of the stratified charge, ignition could be improved. The injection patterns tested consisted of radial, swirl and penetrative. The radial pattern (style A) injected fuel radially toward the spark plug electrode. The swirl pattern (style B) was similar to the radial pattern but had the injection fuel ports offset by 2mm to create a swirl motion of the

fuel injected toward the spark plug electrode. The penetrative pattern (style C) had the injection fuel ports angled down by 15 degrees from the horizontal to push the fuel further into the cylinder. Logan also varied the horizontal location of the PSC injection jets with respect to the spark plug electrode using spacers.

Logan found that by using the inserts with varying injection patterns, the lean limit of combustion could be extended compared to the no-PSC case for engine speeds of 1500 rpm, 2000 rpm and 2500 rpm. This was an improvement over the modified spark plug design used by Reynolds which only saw an extension of the lean limit for engine speeds of 2000 rpm and 2500 rpm[5]. Logan also made the following conclusions taken directly from his Masters thesis[10]:

1. Infeed tube length between the injector and the insert injection location has a large effect on mass flow and injection duration. A shorter length decreases the mass flow variability and shortens the overall injection time. It has also been demonstrated that injection tube dead volume is a significant contributor to post combustion CH4 levels.

2. Concerning the original 14mm spark plug and the 18mm insert designed by David Gorby[11], the best gains are mostly consistently achieved when using a 1mm spacer to offset the location of the electrode in relation to the injected gas. At 2000rpm, it is possible to achieve a relative air fuel ratio of 1.70 versus the homogenous limit of 1.56, BSFC and thermal efficiency improvements of 4% and 1.2% respectively, and brake mean effective pressure (BMEP) improvements of up to 4%. At the extended relative air-fuel ratio, nitrogen oxides (NO_X) values were higher than, but still very close to, the homogenous lean limit values.

3. Concerning the new PSC insert using the 8mm spark plug with the Omega solenoid, the best results in BMEP, NO_X, tHC and CH_4 levels are accomplished through the use of the B style injection pattern. BSFC results are very similar in both A and B pattern injections. It is difficult to decide on an optimal spacer height to associate with the best injection pattern, as both the 1mm and 3mm spacers increases positive results in similar fashions. At 2000rpm, it is possible to achieve a relative air-fuel ratio of 1.67 versus the homogenous limit of 1.47, BSFC and thermal efficiency improvements of 5.7% and 1.7% respectively, and BMEP improvements of up to 9.7%. At the extended relative air-fuel ratio for 2000rpm, NOx were matched to the homogenous lean limit values. At 1500rpm and 2500rpm, it was possible to decrease the NOx values by up to 44% and 71%, respectively.

4. Initial testing with the C style injection pattern using the AFC injection solenoid showed promise in terms of lean limit extension and decreased NOx values. With these preliminary tests, the B style injection pattern still had the best increase in BSFC, thermal efficiency and BMEP.

Although Logan concluded that pattern B was most successful at improving combustion at high λ values, the improvements were minimal and not considered significant enough to be a determining factor when considering which injection pattern to use for the double-PSC-injection method presented in this thesis.

1.1.3 Other Lean-Burn Technologies

There are many other technologies in use today to improve the performance of lean-burn homogenous-charge engines. The following technologies do not require a complete redesign of the engine and are therefore worth presenting for comparison to the PSC method presented in this thesis.

C. Arcoumanis et al. used a partially-stratified charge method similar to the PSC method presented earlier with the exception of the fuel injected at the spark plug being premixed with air with a $\lambda = 1.1$[14, 13]. They found that by having 3.5% of the fuel injected this way they could extend the lean limit of combustion for propane to $\lambda = 1.85$ at an engine speed of 1000 rpm[14]. They also saw a reduction in burn time and an increase in peak in cylinder pressure using their partially-stratified charge method over the homogeneous-charge case.

Varying the design of the piston crown is an option that is relatively cost effective and requires little modification to the engine, although it does require the engine to be disassembled to replace the piston. R. L. Evans has tested a variety of piston crowns in an attempt to increase small scale turbulence thereby increasing flame speed at lean air-fuel ratios for natural gas homogeneous-charge spark-ignited engines[15, 7]. The results of Evans' Squish Jet piston crown design[16] showed improvements in BSFC of 3%, a 5% increase in brake mean effective pressure (BMEP), and an extension of the lean limit of combustion when compared to the bowl in piston design commonly used in lean-burn engines. Evans also found improvements in exhaust emissions including a reduction in brake specific total hydrocarbons (BStHC) of 20% as well as a 50% reduction in brake specific nitrogen oxides ($BSNO_X$)[15].

Rajesh C. Iyer et al. also proposed modifications to the bowl in piston design for natural gas and gasoline fueled homogeneous-charge engines[18]. Iyer ran tests with tapered piston crowns and crescent-shaped cut-outs to see if these designs could increase turbulence inside the engine cylinder. The results for comparing the different designs showed varying results with no obvious choice for the best performing crown geometry. There was, however, improvements shown with regards to increasing the compression ratio for the natural gas fuel engine. The compression ratio was able to be increased from 6.2 to 7.1 when using the design with the crescent-shaped cut-outs while still maintaining good engine performance[18].

Another method employed in lean-burn engines is fuel-enrichment. This method has been used on natural gas engines and involves adding hydrogen to the air-fuel mixture before it enters the combustion chamber[19, 20]. Stuart R. Bell and Manishi Gupta found improvements in engine performance at $\lambda > 1.25$ and extension of the lean limit of combustion. The best improvements in engine performance were found when the fuel supplied was 10-15% hydrogen[19]and included shorter burn durations and less retarded spark timing as well as an extension of the lean limit of combustion.

1.2 Research Objectives

The main objective of the research undertaken in this thesis is to see if using two PSC injections shows any improvements in engine performance over using just one PSC injection for lean air-fuel ratios. There are two reasons why the use of two stratified-charge injections over one may be beneficial. The first is that spreading the fuel injec-

tion over multiple injections has been effective at improving combustion for stratified-charge engines. The second is that in constant-volume combustion bomb experiments performed by Edward Chan[12], using two stratified injections when employing PSC allowed for more complete combustion of the lean bulk charge. It was assumed that the second injection, occurring just after ignition, pushed the flame kernel further into the bomb thereby increasing the flame speed and improving combustion. However, the bomb does not compensate for the effect of charging volume present in an engine nor the effect of having limited combustion time, so engine tests are required.

The secondary objective is to see if the new PSC injection system described in Section 2 can improve combustion and exceed engine performance at lean air-fuel ratios when using only one PSC injection. The new system is expected to offer improved control over the timing and injection mass of the PSC injection. If this is the case, it is expected that the lean limit of combustion will be extended to higher λ values and that there will be decreases in BSFC and COV of IMEP at moderately lean conditions (λ = 1.4-1.65) for engine speeds of 1000 rpm, 1500 rpm and 3000 rpm. The old PSC system had not been tested at engine speeds of 1000 rpm or 3000 rpm and since these speeds are at the extreme ends of the test engine's operational range, there is interest to see if PSC could decrease BSFC and COV of IMEP at these speeds. This would show the effectiveness of the PSC system over the engines full speed range.

Chapter 2

Experimental Set-up

This section covers the most important aspects of the experimental set-up. A more detailed description can be found in Appendix A.

2.1 PSC Set-up

The PSC system consists of a mechanical system and an electrical system which over lap at the fuel injector. On the mechanical side natural gas runs through a compressor where the pressure is raised from 50 psi to approximately 4500 psi. It then passed through two regulators where the pressure is dropped first to 1000 psi then down to the desired injection pressure. The gas is then delivered to the fuel injector via ¼" stainless steel tubing. The fuel injector is held by a custom made support that allows the gas to flow from the tip of the injector into a 1/16" capillary tube. The gas then flows through a check valve, through more ¼" tubing and into the PSC insert. The insert channels the gas toward the electrode of the spark plug installed in the engine. The insert is installed in the spark plug hole in the engine cylinder head.

On the electrical side, a signal is sent from the control room computer to a timing card indicating the length of the injection and when it should occur in reference to the

crank angle. When the specified crank angle is reached the timing card sends a signal to the injector driver telling it how long to open the injector for. The driver sends 100V from the power supply to the injector for the specified injection duration.

For a more detailed description of mechanical and electrical PSC systems see Appendix A Sections A.1 and A.2 respectively.

2.1.1 Spark Plug Insert

The two-piece spark plug insert designed by Logan[10] was used for all experiments preformed. The insert screws into a 14mm spark plug hole in the engine cylinder head and an 8mm spark plug is subsequently screwed into the insert. The insert supplies a small amount of natural gas via a capillary tube and small passages inside the insert to the spark plug electrode.

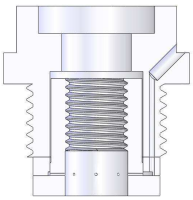

Figure 2.1: PSC Spark Plug Insert[10]

See Appendix A Section A.1.1 for more detail.

2.1.2 Stratified-Charge Injector

The injection system for the stratified-charge had to be changed from the previous set-up in order to accommodate double-injections. Also, the previous system was deemed to have injection opening and closing times that are too slow due to a solenoid valve being used to control the injections. In order to meet the new requirements, a piezo-electric gasoline direct fuel injector was chosen. There were no injectors on the market designed to meet the pressure, volume, and fuel requirements so a compromise was made. A gasoline fuel injector was chosen to meet the requirement of small injection volumes. Since the fuel injector was designed for injecting gasoline, which is far more dense than the natural gas being used, the volume of fuel injected per injection was inline with what was needed for the stratified-charge injection. It is also capable of handling the higher injection pressure required, where a port injector could not, but would still be operating well below the minimum pressure recommended by the manufacturer.

There were concerns as to whether the injector would leak, overheat or freeze due to the use of natural gas vs. gasoline but none of these were an issue during testing. It is possible that if used repeatedly over time these issues could arise, but for the purpose of testing the double-injection concept, this injector was adequate. More detail about the injector as well as injector characterization tests can be found in Appendix A Section A.1.2.

2.2 Engine

2.2.1 Engine Configuration

The engine used for all experiments was a Ricardo Hydra, single-cylinder, two-valve, research engine with the following configuration:

Table 2.1: Engine Specifications

Compression Ratio	10.2	Intake Valve Open	12 deg BTDC
Bore	80.26 mm	Intake Valve Close	56 deg ABDC
Stroke	88.90 mm	Exhaust Valve Open	56 deg BBDC
Connecting Rod Length	158.00 mm	Exhaust Valve Close	12 deg ATDC
Swept Volume	450 cc		
Clearance Volume	48.97 cc		

2.2.2 Spark Plug Specifications

An 8mm NGK ER9EH spark plug, with the specifications listed below, was used for all experiments.

Table 2.2: Spark Plug Specifications

Ground Electrode Thickness	Spark Gap	Central Electrode Diameter	Electrode Type
0.030”	0.027”	0.060”	Flat

2.2.3 Piston Specifications

A bowl in piston design, the same as that used by Eric Kastanis in his M.A.Sc. thesis[21], was used for all tests. The reasoning for its use was simply because it was a bowl in

piston design and was readily available. The piston was scaled from a 137 mm bore Caterpillar G3406 and has a bowl volume is 25.26 cc resulting in a clearance volume of 48.97 cc.

2.2.4 Homogeneous-Charge Fuel Supply

The bulk charge for all tests performed was a premixed homogeneous-charge resulting from the mixture of the engine test cell air and standard supply natural gas. The natural gas used was from the same source as the PSC fuel supply but was used directly from the natural gas line without having the pressure increased using the compressor. This fuel source had an approximate pressure of 50 psi. The fuel composition can be found in Appendix A Section A.4.

2.3 Data Acquisition Systems (DAQ)

The engine is equipped with both high-speed and low-speed sampling instrumentation. High-speed sampling of the in-cylinder pressure happens at 1440 samples per engine cycle and is averaged over 100 cycles. Low-speed sampling of all temperatures, non-in-cylinder pressures, exhaust emissions, engine performance measurements, fuel mass and air volume flow, happen at approximately 80 samples per minute and are averaged over 100 samples. Measurement devices and their uncertainties can be found in Appendix C.

Chapter 3

Experimental Results and Discussion

The purpose of this thesis is to examine the effects of double-injection-PSC vs. single-injection-PSC as well as to compare the results to the baseline no-PSC case. Since new apparatus was used for the tests, it is important to first find the optimum operating conditions for the single-pulse-injection (SPI) PSC cases. After that, the bulk of the testing was performed to find the optimum operating conditions for the double-pulse-injection (DPI) PSC cases. Further investigation was required at $\lambda > 1.65$ to determine the mechanism of the extension of the lean limit and this data is presented in its own section.

3.1 Methodology

On testing days the engine was started, warmed up and operated following the Engine Operating Procedures found in Appendix D. To reduce errors in the data due to varying air and fuel conditions, all tests that were to be compared were performed on same day. The individual tests in these sets were also preformed at random to reduce any errors

due to the engine having not stabilized for the given test point. This was a secondary measure used in addition to waiting for engine emissions to stabilize before taking data for a given test point.

Spark timing was chosen using the minimum advance for best torque technique described in Appendix E. All tests were performed at wide open throttle. All values presented were calculated using formulas from Haywood[4] and are also available in Appendix B. Details of experimental techniques specific to a particular set of test are given in the following sections along with the test results.

3.2 Preliminary Single-Injection-PSC Optimization Tests

It was important to find the optimum operating conditions for the single-injection tests in order to determine whether double-injection-PSC could offer an improvement over single-injection. To do this, tests were first performed at given engine speed for an intermediate λ value (λ=1.55) where the benefits of single-injection-PSC over no-PSC had previously been seen. A variety of PSC fuel pressures, injection timings and injection pulse-widths were tested and the results for both brake specific fuel consumption (BSFC) and coefficient of variation of indicated mean effective pressure (COV of IMEP) were plotted and compared. BSFC and COV of IMEP were chosen because they are both good indicators of engine performance. The conditions giving the lowest BSFC and COV of IMEP were picked for further testing, limiting the test conditions to 4-6.

Testing was performed using those test conditions over a range of λ values (1.3-1.65). Again the results for BSFC and COV of IMEP were plotted and compared. The test condition that gave the lowest BSFC and COV of IMEP over the widest range of λ was chosen as the optimum single-injection-PSC operating conditions for the engine speed for which the tests were run.

During testing there were some unforeseen issues with spark timing requiring additional tests to be run. Although MBT spark timing was determined for each test point, there was some error in determining this value. Since there is a strong dependence between spark timing and engine performance, tests were redone with a constant spark timing for a given λ value. This allowed the effects of varying PCS injection conditions to be fairly evaluated. Spark timing for non-PSC tests were determine separately since more advanced spark timing was required due to the slower flame speed.

There were some test conditions that couldn't be run due to extremely poor engine operation at these conditions. Originally, the plan was to test 3 PSC pressures (32, 24 and 16 bar) for engine speeds of 1000, 1500 and 3000 rpm. These pressures were chosen because they had been tested before with the previous PSC apparatus. The engine speeds were chosen as a high (3000 rpm) and low (1000 rpm) speed for the engine plus an intermediate speed (1500 rpm) where the engine and dynomometer system runs most efficiently.

The 32 bar pressure was found to give too high of a PSC flow rate even at a short 1ms injection-pulse-width and was not including in testing at any of the engine speeds. A PSC injection pressure of 8 bar was added to testing at all engine speeds to keep the variety in pressures while investigating the possibility of using a lower injection pres-

sure than had been proven to be optimal using the previous PSC apparatus. Previous testing had shown 16 bar to be the optimal PSC injection pressure.

At 1500 rpm, the PSC injection pressures of 8, 16 and 24 bar seemed to work well with all pressures offering combustion improvements, lower BSFC and COV of IMEP, over the no-PSC case.

At 1000 rpm, high-pressure PSC injections were a problem so tests were performed at lower pressures of 8, 12 and 16 bar. Since the total fuel flow rate is lower at a given λ value at 1000 rpm than at 1500 rpm, if a high PSC injection pressure is used, even when using small injection-pulse-widths, the percent PSC flow rate with respect to the total fuel flow rate is quiet high. As a result the λ value for the bulk charge becomes quiet high and even with the PSC injection, the engine performance is poor.

At 3000 rpm, the negative impact of having too large a PSC injection was very pronounced and PSC pressures of 6, 8 and 12 bar were used instead. The cause of these issues could be due to the earlier spark timing required at 3000 rpm for a given λ compared to that at 1500 rpm. This means the cylinder pressure into which the PSC fuel is being injected is lower, giving a high pressure difference and therefore a higher PSC flow rate. This high flow rate could cause the air-fuel ratio near the spark plug to be too rich for ignition.

3.2.1 Example of Preliminary Testing: 1500 rpm Engine Speed

The following graphs are presented of an example of the data gathered for the first stage of the preliminary testing. These test were performed at 1500 rpm, λ = 1.55 and a PSC injection pressure of 8 bar. Note that the injection timing is plotted in terms of

crank angle degrees. At 1500 rpm, 9 degrees = 1ms.

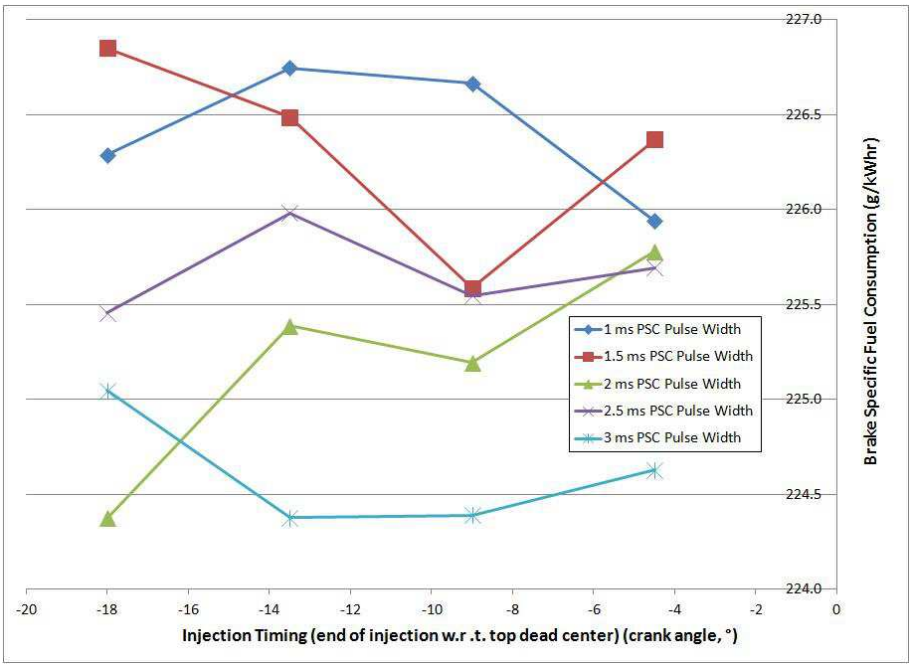

Figure 3.1: First Stage Preliminary Tests BSFC: 1500 rpm, λ = 1.55, 8 bar

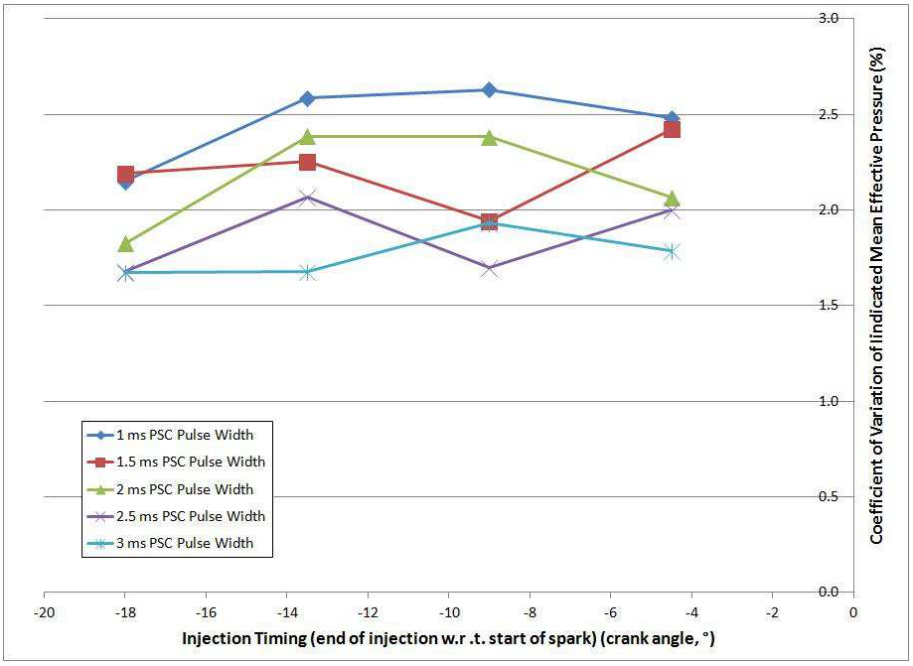

Figure 3.2: First Stage Preliminary Tests COV of IMEP: 1500 rpm, λ = 1.55, 8 bar

The data from the previous two graphs, along with data for 16 and 24 bar PSC injection pressures was used to determine which PSC injection conditions gave the best engine performance. Since low BSFC and COV of IMEP are commonly used as indicators of good engine performance, the conditions that produced the lowest BSFC and COV of IMEP were chosen for further investigation. These PSC-injection conditions chosen were as follows: 8-bar-pressure ending 1-ms-before-spark with durations of 2, 2.5 and 3 ms, 16-bar-pressure ending 1.5-ms-before-spark with durations of 1, 1.5, 2 and 2.5 ms. To see if λ had an effect on the comparative engine performance, tests were performed for λ= 1.3-1.75 using these PSC injection conditions.

The data for λ= 1.3-1.75 was analyzed for engine performance by looking at the

data for each λ value separately. The following graphs are presented as an example of this data. Tests preformed at a PSC-injection-pressure of 8 bar have PSC injections ending 1-ms-before-the-start of spark. Tests preformed at a PSC-injection-pressure of 16 bar have PSC injections ending 1.5-ms-before-the-start of spark. Note that the injection duration is plotted in terms of crank-angle degrees. At 1500 rpm, 9 degrees = 1 ms.

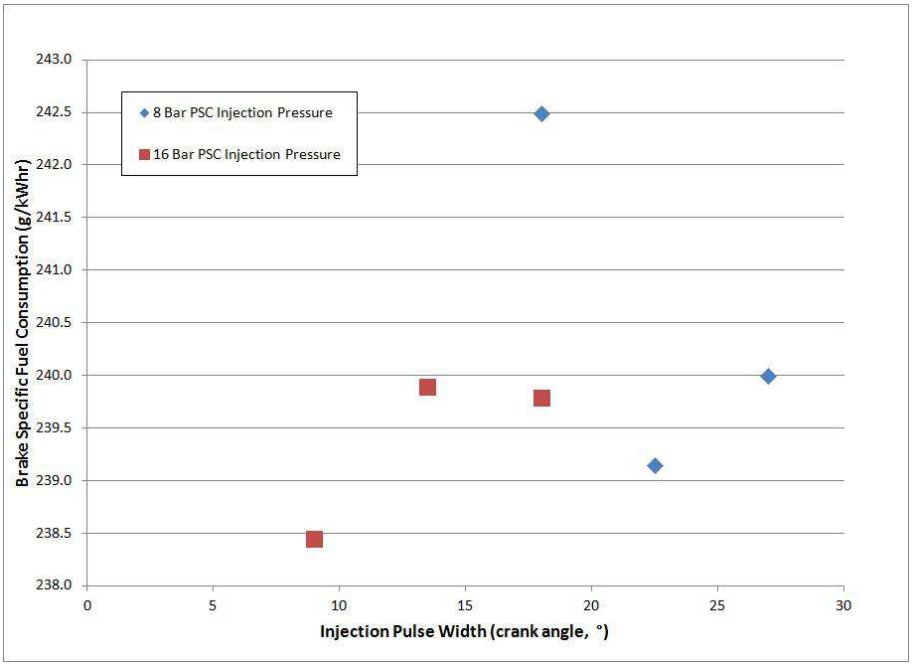

Figure 3.3: Second Stage Preliminary Tests BSFC: 1500 rpm, λ = 1.65

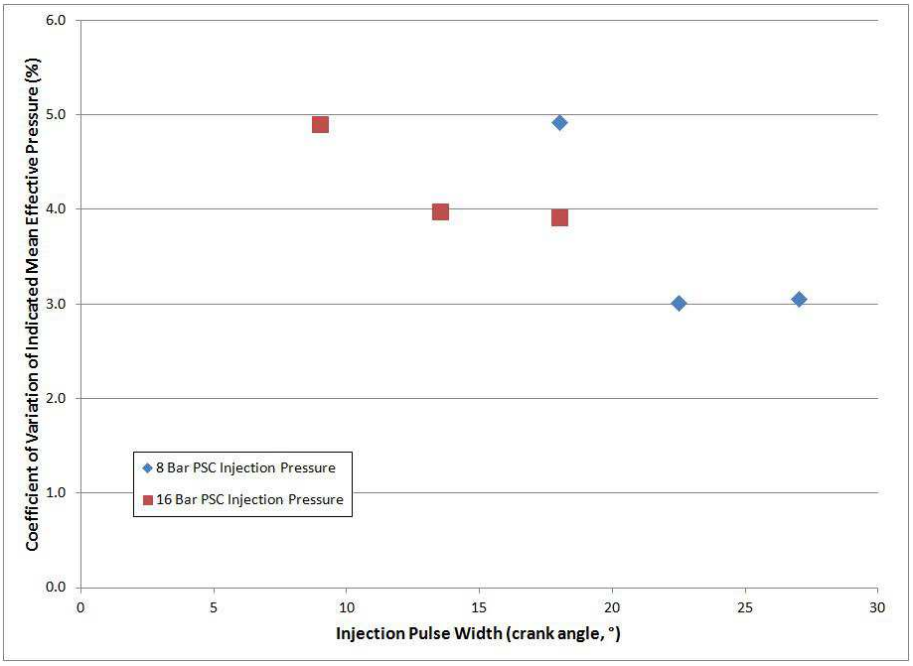

Figure 3.4: Second Stage Preliminary Tests COV of IMEP: 1500 rpm, λ = 1.65

The results of the graphs shown, as well as the graphs for other λ values, show the PSC-injection condition with the lowest BSFC and COV of IMEP over the range of λ= 1.3-1.75 is most consistently that having a pressure of 16 bar, a pulse-width of 1.5 ms and a timing of 1.5 ms before-the-start of spark for single-injection-PSC at 1500 rpm. These parameters were used for the single-injection data that is compared to the double-injection data shown in the next section.

3.2.2 Optimum Single-Injection-PSC

The following table shows the operating parameters that gave the best engine performance (lowest BSFC and COV of IMEP) for single-injection-PSC for a given engine

speed.

Table 3.1: Optimum Engine Performance Parameters for Single-Injection-PSC

Engine Speed (rpm)	Injection Pressure (bar)	Injection Pulse Width (ms)	Injection Timing (end of injection w.r.t. start of spark in ms)
1000	12	2	1.5
1500	16	1.5	1.5
3000	6	2	0.5

3.3 Main Double-Injection-PSC Tests

The theory as to how a second PSC injection could improve combustion was that the second injection would push the flame kernel, created by the first injection, further into the engine cylinder then if there was only one injection. To test this theory, a second injection was added after the single-injection that had produced the best engine performance in the preliminary test. The PSC system was designed to have only one fuel supply for the PSC injector in order to minimize the complexity of the apparatus, and as a result the PSC injection pressure had to be the same for both injections. The duration of the second injection was varied between 1 and 4 ms and the timing of the start of the second injection was varied between 0 and 4 ms after the end of spark. The spark timing was the same as that used for the preliminary tests. Note that the abbreviation in the graph legends presented in this section SPI and DPI, stand for single-pulse-injection (or single-PSC-injection) and double-pulse-injection (or double-PSC-injection) respectively.

3.3.1 1500 rpm Double-Injection-PSC Tests

Tests were performed using double-PSC-injections with pulse widths of 1 and 3 ms starting 0, 2 and 4 ms after the end of spark. All PSC tests were performed with a PSC pressure of 16 bar. All single-PSC-injections as well as all primary injections for double-PSC-injection cases had a 1.5 ms pulse-width with the injection ending 1.5-ms-before-the-start of spark. The pulse lengths and timings for the data series labeled as DPI in the graph legends, refer to the secondary PSC injection.

As a reference the flowing table is presented to give estimations of the PSC injection flow rates and the percent of the total fuel flow rate that is from the PSC injection flow rate, for the PSC injection conditions used in the 1500 rpm tests.

Table 3.2: PSC Flow Rates at 1500 rpm

PSC Injection Type	Total PSC Injection Pulse Width (ms)	Total PSC Injection Flow Rate (g/hr)	Percent PSC of Total Fuel at λ = 1.65
Single-PSC-Injection	1.5	13	1.9%
Double-PSC-Injection 1 ms Secondary Injection Pulse	2.5	21	3.1%
Double-PSC-Injection 3 ms Secondary Injection Pulse	4.5	39	6.0%

In order to be able to visualizes the various injection timings used the timing diagram in Figure 3.5 shows the timing of the fuel injection events together with the ignition timing relative to top-dead-centre (TDC). All timings are shown for λ= 1.75 at 1500 rpm.

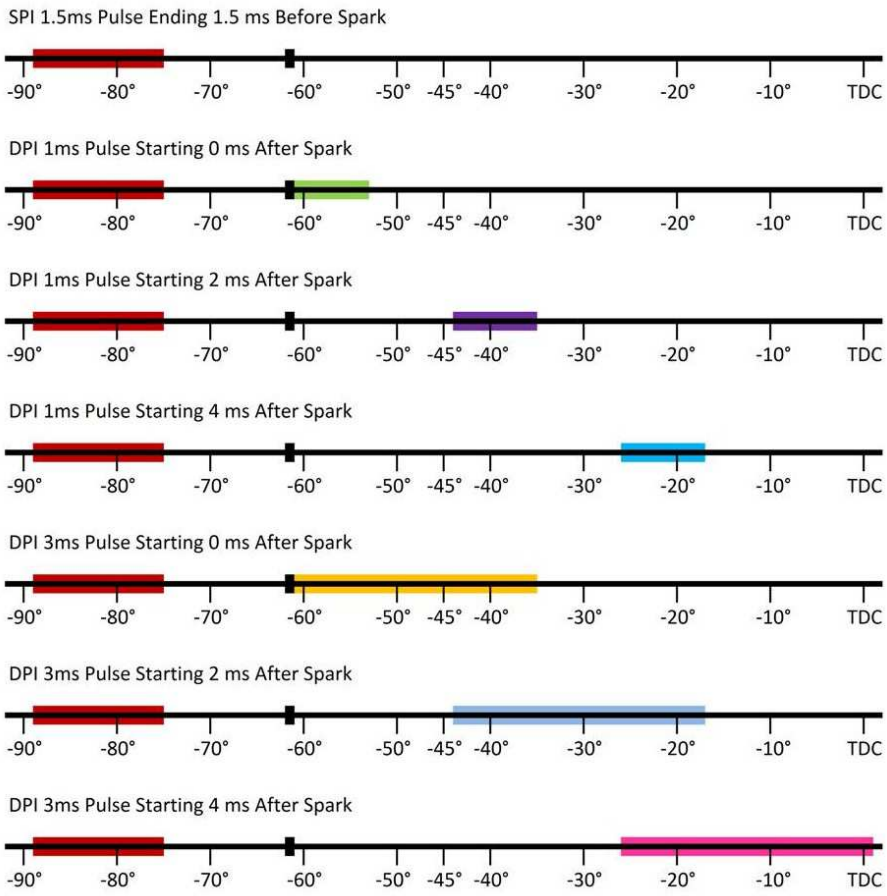

Figure 3.5: Injection Timing Diagram:λ= 1.75, 1500 rpm

The small black rectangle shows where the spark occurs, while all red rectangles show the timing and duration of the primary injection and the other coloured rectangles show the secondary injection events. The secondary injection events are colour coded to match the same conditions on the graphs in the subsequent figures.

The following graph is shown as an example of the results for tests with λ ranging

from 1.3 to 1.75. All graphs showed little variation between no-PSC and single and double-PSC-injection for λ = 1.3 - 1.5. As a result, the rest of the data is only be presented for λ= 1.55 - 1.75 so that the data can be more clearly represented on the graphs.

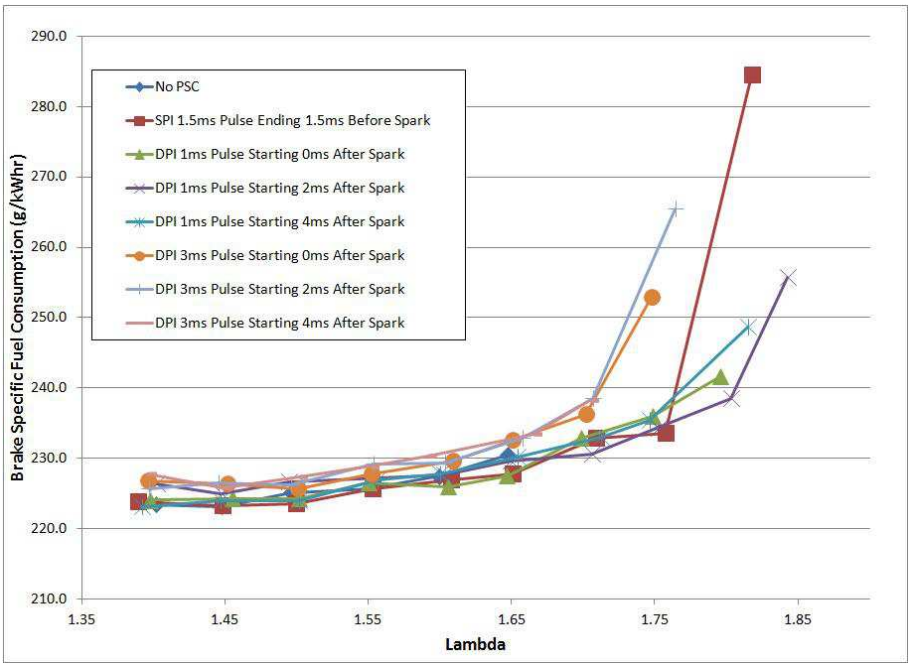

Figure 3.6: DPI - BSFC vs.λ= 1.3-1.85 at 1500 rpm

The following graphs shows BSFC, COV of IMEP, thermal efficiency, brake specific methane ($BSCH_4$) and brake specific nitrogen oxides ($BSNO_X$) for double-PSC-injection data, optimum single-PSC-injection and the no-PSC baseline, for 1500 rpm and λ = 1.55 - 1.85. Not all test conditions could be performed at all λ values. At λ = 1.7 and higher, the engine was not able to operate without some form of PSC injection.

This was also the case for the 3-ms-pulse-width double-PSC-injection cases at λ = 1.8 and higher. There is no data for the double-PSC-injection 3-ms-pulse-width starting 4-ms-after-spark case for λ > 1.7 due to this test point being missed on the day the rest of the tests were performed.

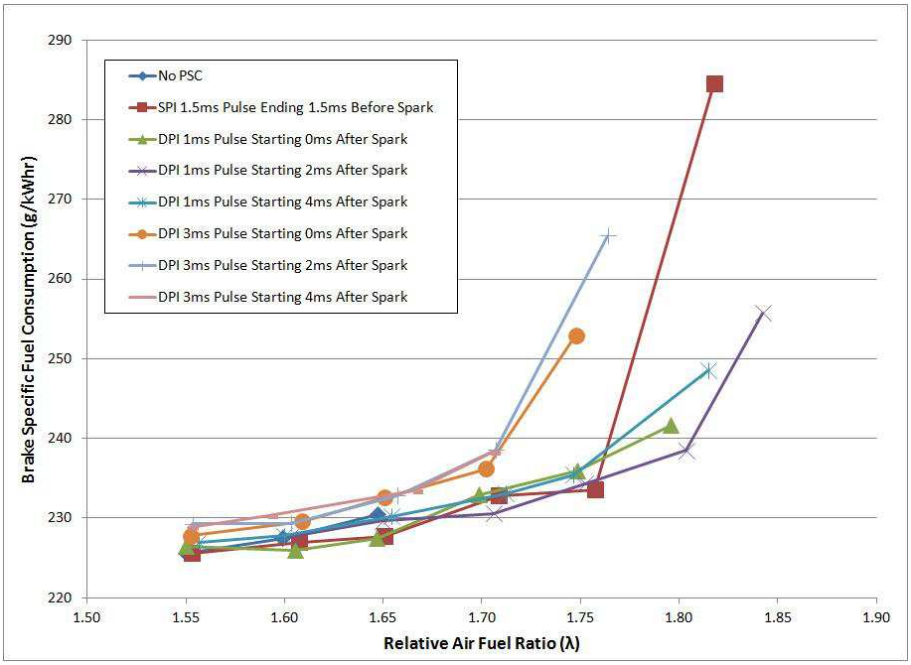

Figure 3.7: DPI - BSFC vs.λ= 1.55-1.85 at 1500 rpm

The graph for BSFC shows no significant benefit of PSC injection until λ is greater than 1.65 at which point PSC injection allows the engine to continue to operate. All 3-ms-pulse-width double-PSC-injection cases show higher BSFC than the single-PSC-injection and 1-ms-pulse-width double-PSC-injection cases, indicating that not all of the secondary PSC injection is being burned efficiently when there is a

higher secondary PSC injection fuel flow rate. The 1-ms-pulse-width double-PSC-injection cases give the same BSFC results, within error, as the single-PSC-injection case for $\lambda \leq 1.75$. For $\lambda > 1.75$ the double-PSC-injection cases with a secondary-pulse-width of 1 ms shows improvement over the single-injection case. This may, however, be due to the increase in total PSC flow rate rather than the addition of a second PSC injection and is investigated further in Section 3.4.

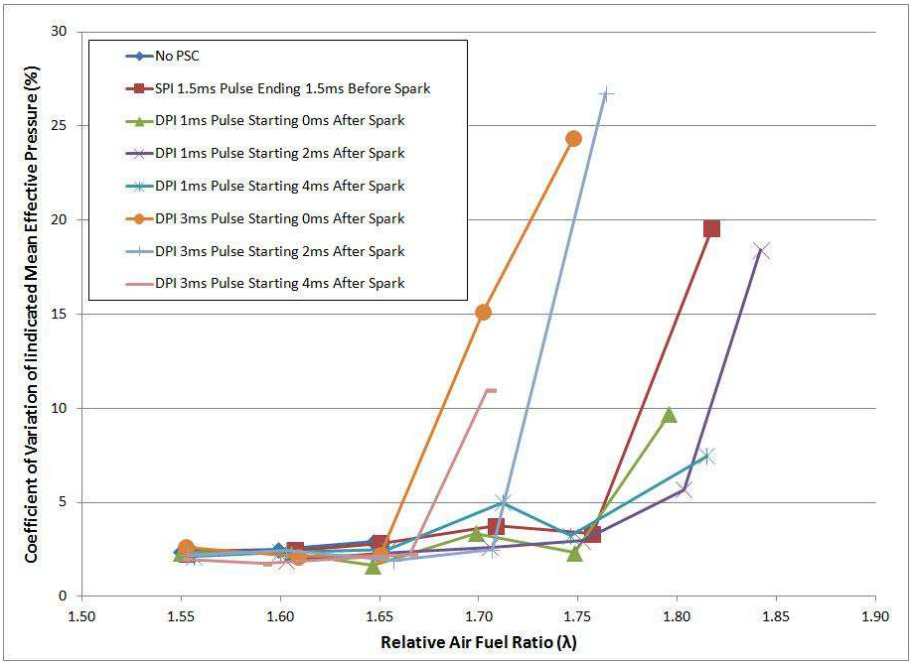

Figure 3.8: DPI - COV of IMEP vs.λ= 1.55-1.85 at 1500 rpm

The COV of IMEP graph shows similar results to the BSFC graph and the same reasoning can be applied with respect to an explanation. With regards to the 3 ms pulse width double-PSC-injection cases showing higher COV of IMEP than the

single-PSC-injection and 1 ms pulse width double-PSC-injection cases, if not all of the secondary PSC injection is being burned efficiently due to the higher secondary PSC injection fuel flow rates, as hypothesized earlier, this could be due to a rich air-fuel ratio zone being created by the secondary PSC injection. This rich air-fuel ratio zone would stall combustion and cause more cycle to cycle variation and a higher COV of IMEP.

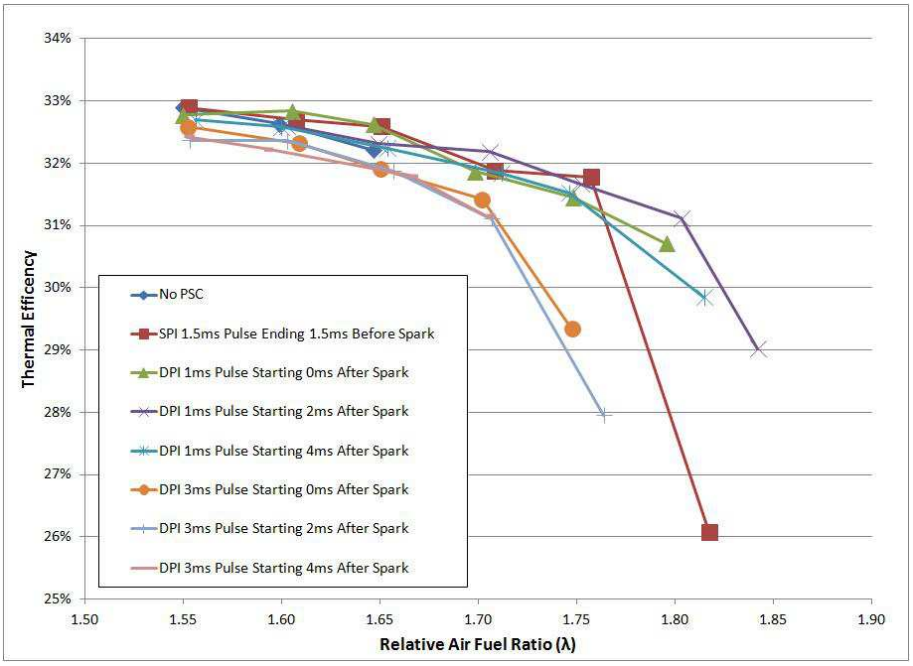

Figure 3.9: DPI - Thermal Efficiency vs.λ = 1.55-1.85 at 1500 rpm

Again, the data trends seen in the BSFC and COV of IMEP can be seen in the thermal efficiency data. The trends in thermal efficiency follows those of the BSFC data, only inverted, as expected. The thermal efficiency graph is presented more as a reference

than as a means of conveying more information.

The following graphs show the IMEP and when the maximum cylinder pressure occurred with respect to TDC for each of the 100 cycles measured at the given test points.

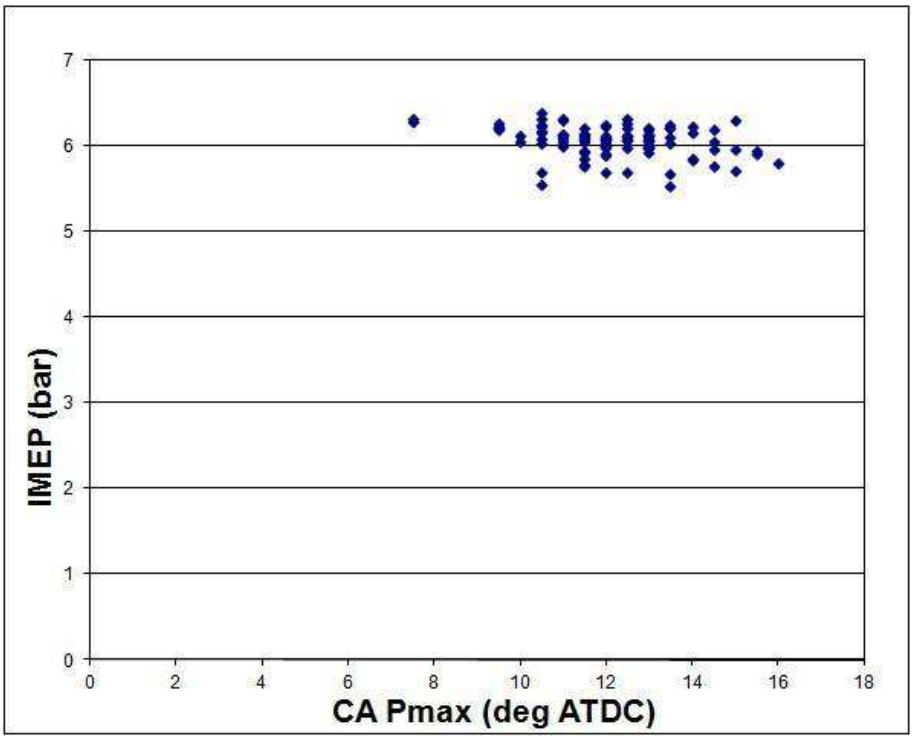

Figure 3.10: IMEP vs CA of Maximum Pressure for No-PSC: 1500 rpm, λ = 1.65

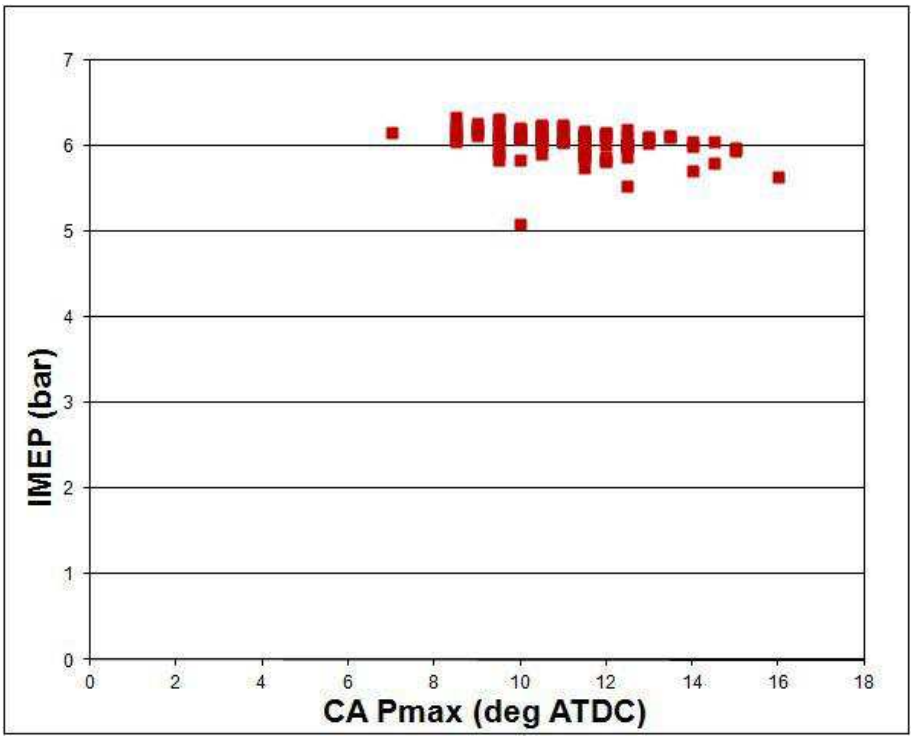

Figure 3.11: IMEP vs CA of Maximum Pressure for SPI: 1500 rpm, λ = 1.65

The IMEP graphs show very little difference between the no-PSC and the single-injection-PSC cases at λ = 1.65. There are no misfires for either case indicating that the COV of IMEP values of 2.8% shown earlier are due to the variation between cycles and not due to just a few misfires with most cycles having a lower variation from the mean.

Integrated heat release curves, which show the timing and rate of combustion, provide another way of looking at the performance differences between various test conditions. Figure 3.12 shows the integrated heat release as a function of crank-angle for

both single-pulse injection and the no-PSC case at 1500 rpm and λ =1.65. These curves were generated by integrating the heat release curves for the average of 100 individual cycles.

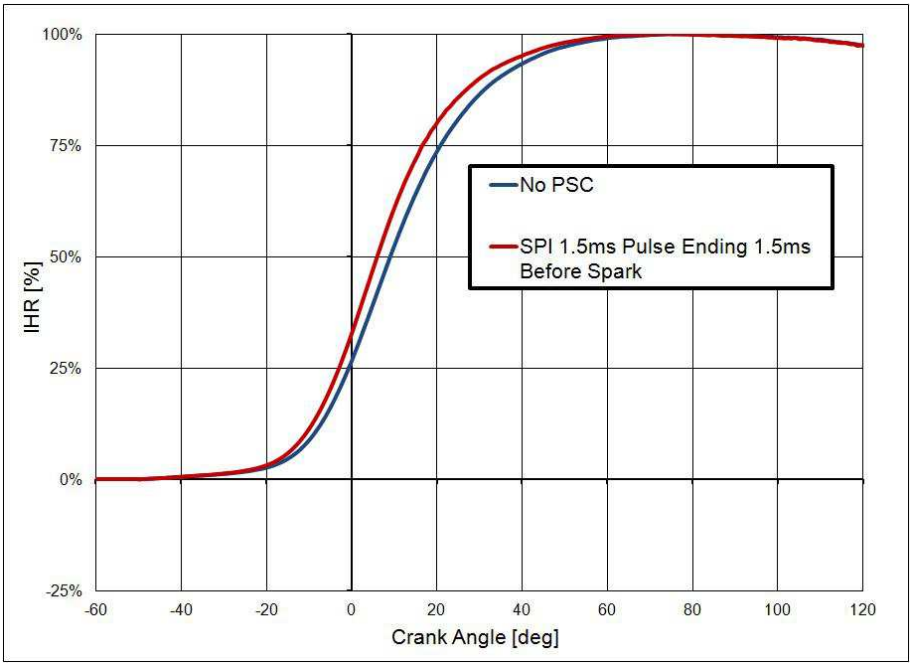

Figure 3.12: Integrated Heat Release vs. Crank Angle: 1500 rpm, λ = 1.65

Although there is no variation in COV of IMEP between the no-PSC and single-PSC-injection case at λ = 1.65, it can be seen that the PSC injection has increased the speed of combustion slightly. This is also shown as a slight improvement in BSFC, compared to the no-PSC case, earlier in this section. More integrated heat release curves are shown in Section 3.4 for higher λ values.

To determine why the double-PSC-injection cases with 3-ms-pulse secondary-injections

perform poorly at high λ values, the following graph is presented.

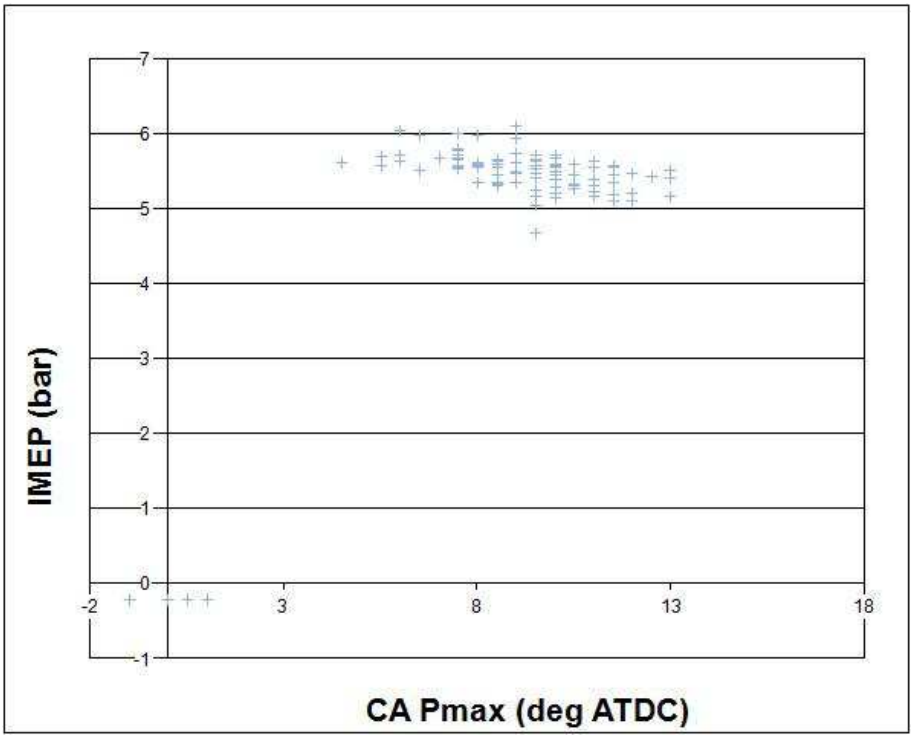

Figure 3.13: IMEP vs CA of Maximum Pressure for DPI 3ms Pulse Starting 2ms After Spark: 1500 rpm, λ = 1.75

For the double-PSC-injection case with a 3-ms-pulse secondary-injection starting 2-ms-after-spark, 6% of the cycles are misfires. At high λ values the PSC injections occur earlier in the compression cycle due to the need for earlier spark timing, and the cylinder pressure is therefore at the time of injection. As a result, more fuel is injected for a given pulse-width. This is likely the reason that the engine performance for the cases with a 3-ms-pulse-width secondary-injection deteriorates. At higher λ values the extra fuel in creates an area around the spark plug electrode that is too rich for ignition.

More IMEP vs. CA for maximum pressure graphs are shown in Section 3.4 for higher λ values where the COV of IMEP becomes much higher.

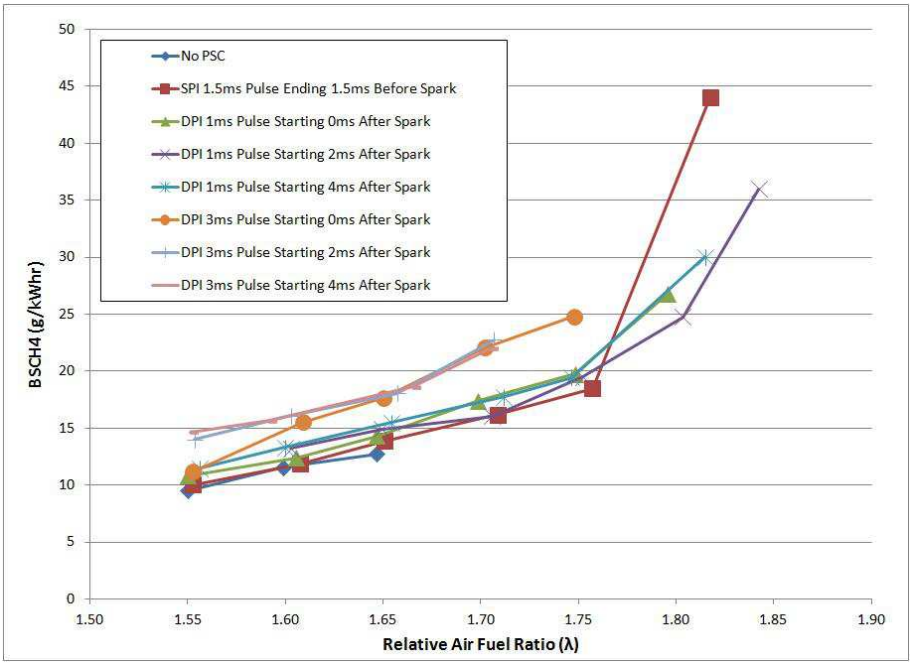

Figure 3.14: DPI - $BSCH_4$ vs.λ = 1.55-1.85 at 1500 rpm

The $BSCH_4$ graph shows an increase in methane emissions for all 3 ms pulse width double-PSC-injection cases over the single-PSC-injection and 1-ms-pulse-width double-PSC-injection cases, validating the hypothesis that not all of the secondary PSC injection is being burned. In all PSC cases the $BSCH_4$ is the same or greater than the no-PSC case for λ values up to and including 1.65. At λ values greater than 1.65 the engine is unable to operate without some form of PSC injection and this is where the benefit of using PSC injection can first be seen. For the case of the

single-PSC-injection and the double-PSC-injection cases with a 1-ms-pulse-width, the BSFC is the same as the no-PSC case, indicating that while less of the fuel is being burned in these PSC cases, the fuel that is being burned is being burned more efficiently. This may be due to the PSC cases not requiring as advanced spark timings as the no-PSC case.

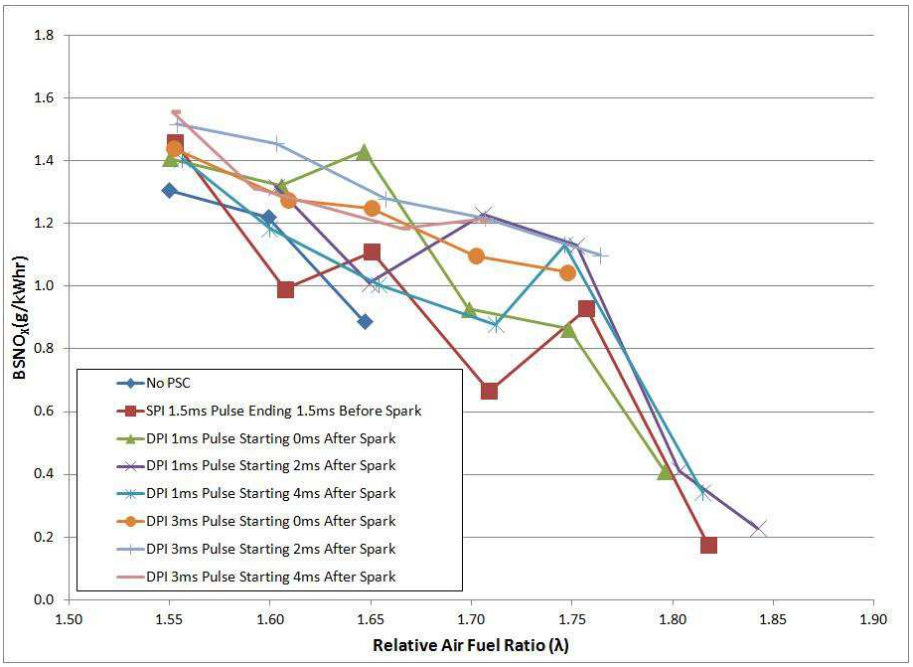

Figure 3.15: DPI - $BSNO_X$ vs.λ= 1.55-1.85 at 1500 rpm

The $BSNO_X$ graph highlights the errors in picking the correct MBT spark timing. This is due to the small values for $BSNO_X$ which allow for less variation in the values. When the errors are considered the data for the different cases mostly fall within the error bounds of the other cases. Not much information can be obtained from the graph

as a result, except that the $BSNO_X$ decreases with increasing λ, as expected, due to the engine running cooler.

The important results for the 1500 rpm test are presented in Section 3.4 after the presentation and discussion of the results of the λ = 1.7 - 1.85 tests.

3.3.2 3000 rpm Double-Injection-PSC Tests

The following tests were performed using double-PSC-injection with pulse-widths of 1 and 2 ms and timings of 0, 1 and 2-ms-after-the-end-of-spark. Larger pulse-widths at more delayed timing were attempted but combustion was so poor that no usable data was obtained. All PSC tests were performed with a PSC-injection pressure of 6 bar. All single-PSC injections, as well as all primary injections for double-PSC-injection cases, had a 2-ms-pulse-width with the injection ending 0.5-ms-before-the-start-of-spark. The pulse-lengths and timings for the data series labeled as DPI in the graph legends, refer to the secondary PSC injection.

Tests were performed at 2900 rpm (3000 rpm nominally) due to problems with the dynomometer system which was unable to provide a stable load at 3000 rpm. At 2900 rpm a stable load was easily achieved by the dynomometer. Preliminary tests were performed at 3000 rpm as there were no issues with the equipment at that time. All tests for the data presented below, no-PSC, single-PSC-injection and double-PSC-injection, were run on the same day at 2900 rpm to ensure no errors when comparing the data. All PSC tests were performed with a PSC pressure of 6 bar.

As a reference the following table is presented to give the PSC injection flow rates and the percent of the total fuel flow rate that is from the PSC injection flow rate, for

the PSC injection conditions used in the 3000 rpm tests.

Table 3.3: PSC Flow Rates at 3000 rpm

PSC Injection Type	Total PSC Injection Pulse Width (ms)	Total PSC Injection Flow Rate (g/hr)	Percent PSC of Total Fuel at λ = 1.65
single-PSC-injection	2.0	13	1.3%
Double-PSC-Injection 1 ms Secondary Injection Pulse	3.0	20	2.0%
Double-PSC-Injection 2 ms Secondary Injection Pulse	4.0	27	2.7%

Figure 3.16 shows the PSC injection and timing diagram for λ = 1.70 at 3000 rpm.

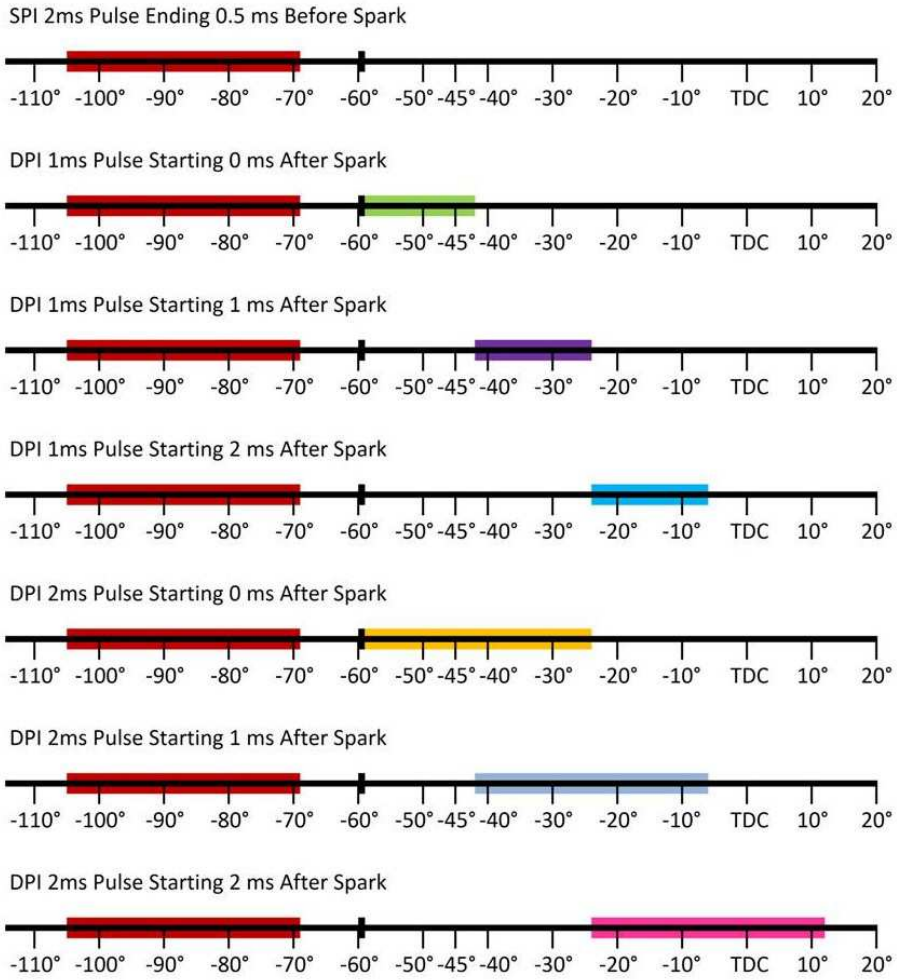

Figure 3.16: Injection Timing Diagram:λ= 1.70, 3000 rpm

The black rectangle shows where the spark occurs, all red rectangles show when the primary injection is happening and the other coloured rectangles show the secondary injections and are color coded to match the same conditions on the following graphs.

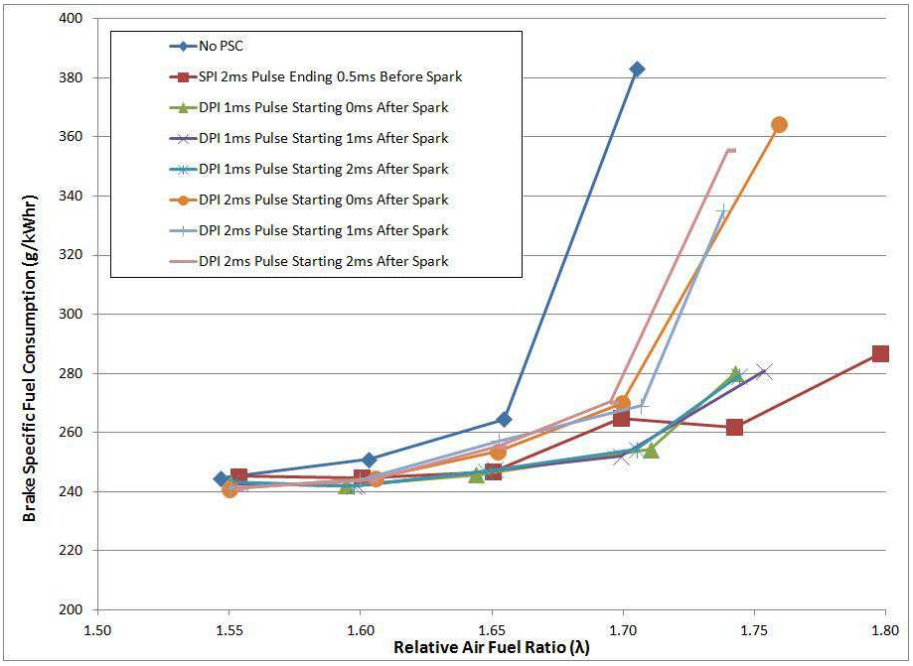

Figure 3.17: DPI - BSFC vs.λ= 1.55-1.75 at 3000 rpm

The BSFC graph shows improvement over the no-PSC case for all PSC cases starting at λ = 1.60. The benefit of the PSC system is realized at lower λ values because at 3000 rpm the air-fuel mixture has half the burn time available compared to 1500rpm. Since the time require for 90% of the air fuel mixture to be combusted (time to get from 5% to 95% on the integrated heat release curve) for a given λ value is not halved between 1500 and 3000 rpm (6.3 ms at 1500 rpm and 4 ms at 3000 rpm for the no-PSC case at λ = 1.65) to compensate for the doubling in engine speed, the engine performance decreases more quickly with increasing λ value at 3000 rpm.

There is no data available for any of the double-PSC-injection cases above λ = 1.75

because the engine would not run under those conditions. Again, the data does not show improvement in BSFC when using any of the double-PSC-injection conditions compared to the single-PSC-injection case. This does not necessarily indicate that there are no double-PSC-injection conditions that would give better BSFC results than the single-PSC-injection case, only that the double-PSC-injection conditions used do not.

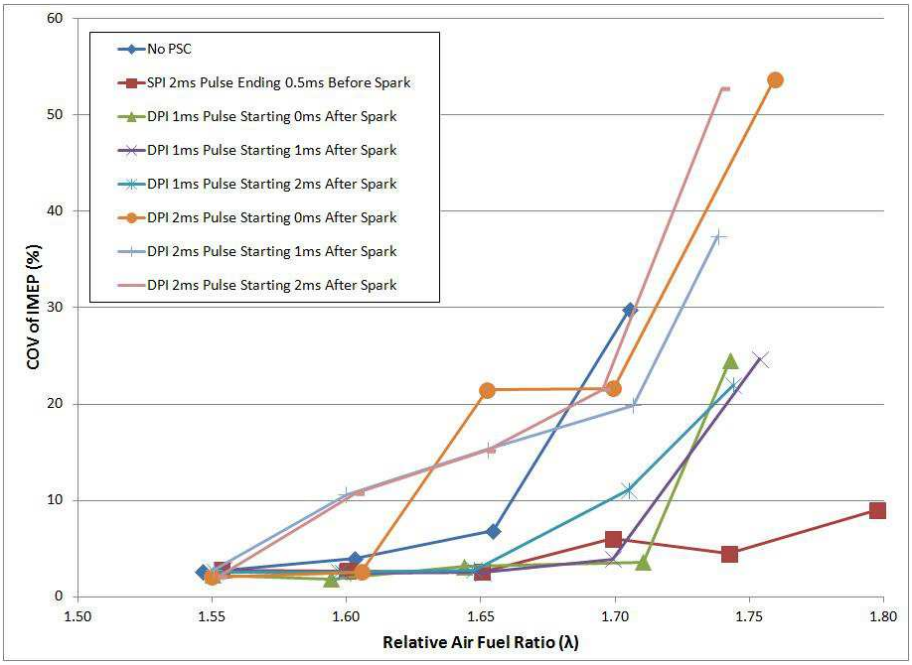

Figure 3.18: DPI - COV of IMEP vs.λ= 1.55-1.75 at 3000 rpm

The COV of IMEP graph shows improvement over the no-PSC case when using single-PSC-injection or 1-ms-pulse-width double-PSC-injection over the no-PSC case for λ greater than 1.55. At λ = 1.60 the double-PSC-injection case with a

2-ms-secondary-injection pulse starting 0-ms-after-the-end-of-spark also shows improvement over the no-PSC case but only at λ = 1.60. As is the case for BSFC, the effects of PSC are realized earlier due to the limited combustion time available for an engine speed of 3000 rpm. Unlike for BSFC, the higher flow double-PSC-injection cases (2-ms-secondary-pulse-width) show higher COV of IMEP. This may be the result of the rich air-fuel ratio condition created by the secondary injection interfering with proper combustion, much like what was seen in the 1500 rpm tests, but only intermittently instead of more regularly. The difference is likely due the injection timing. At 3000 rpm a given PSC injection-pulse-width injects over twice the proportion of the compression stroke than at 1500 rpm. For example, the 2-ms-secondary-PSC-injection pulse used at 3000 rpm injects over 36ºCA (crank angle degrees) where as the 3-ms-secondary-PSC-injection pulse used at 1500 rpm injects over 27ºCA. The longer injection period, in terms of crank angle degrees, allows the injection to be dispersed more and therefore less likely to form an area with an air-fuel ratio too rich to burn. But when this does occur it has a dramatic effect on combustion due to the limited combustion time.

The COV of IMEP graph also shows the single-PSC-injection case being able to maintain a lower than 10% COV of IMEP at λ = 1.80 which is an improvement over the previous PSC apparatus.

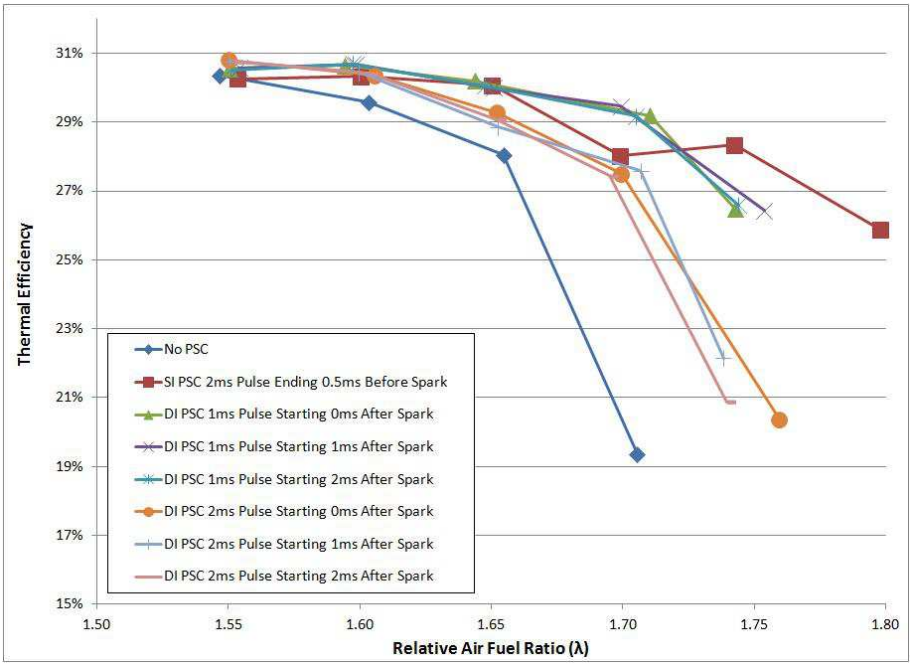

Figure 3.19: DPI - Thermal Efficiency vs.λ= 1.55-1.75 at 3000 rpm

The trends in thermal efficiency follows those of the BSFC data, only inverted, as expected. Again, the thermal efficiency graph is presented more as a reference than as a means of conveying more information.

Figures 3.20 and 3.21 show the IMEP and crank-angle of maximum cylinder pressure with respect to TDC for each of the 100 cycles measured for both the no-PSC case and the SPI case at 3000 rpm and λ =1.65.

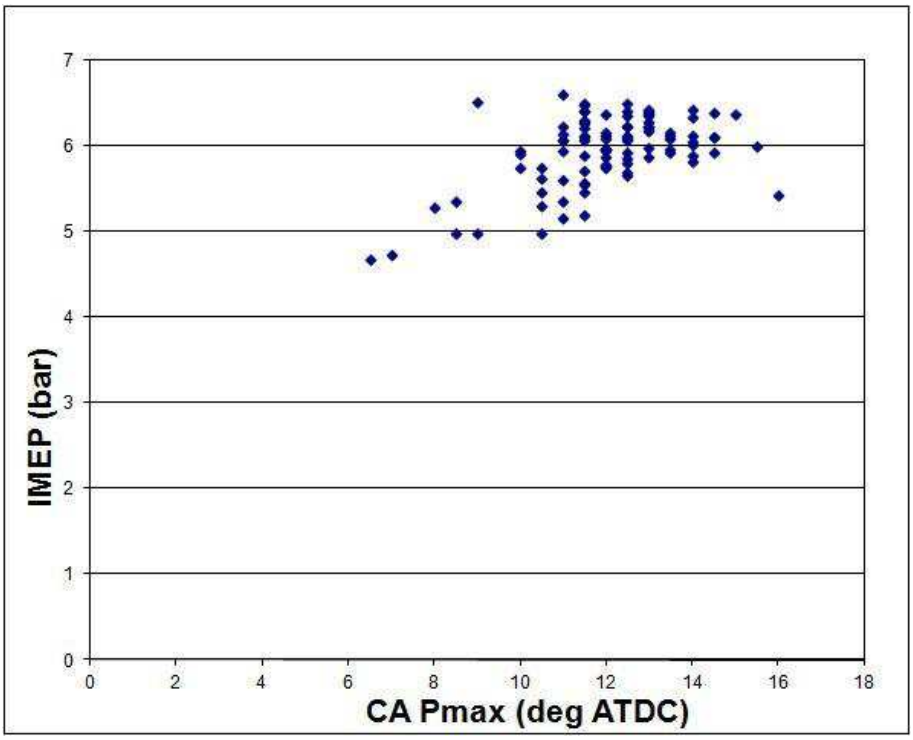

Figure 3.20: IMEP vs CA of Maximum Pressure for No-PSC: 3000 rpm, λ = 1.65

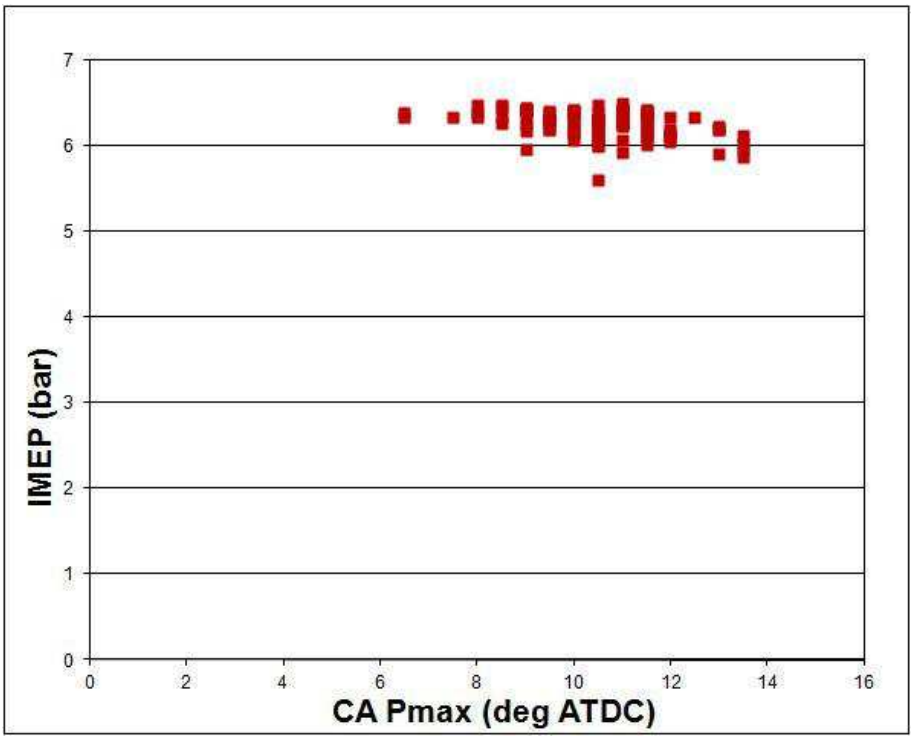

Figure 3.21: IMEP vs CA of Maximum Pressure for SPI: 3000 rpm, λ = 1.65

The IMEP graphs above show the effect of using a single-PSC-injection at λ = 1.65. There are no misfires for either case but the single-PSC-injection case shows much less variation in IMEP. For the no-PSC case the data point are spread out quite evenly for a range of IMEP of 4.6 - 6.6 bar while the single-PSC-injection case varies from 5.5 - 6.5 bar with all but one cycle above 5.8 bar and around 85% of cycles above 6 bar. For the no-PSC case more than half the cycles are below 6 bar. This shows that before the lean limit of combustion for the no-PSC case, PSC is able to improve combustion, even when there are no issues with ignition.

The integrated heat release curves for the cases just presented are shown in Figure 3.22 to see if there are any differences in the speed and timing of combustion.

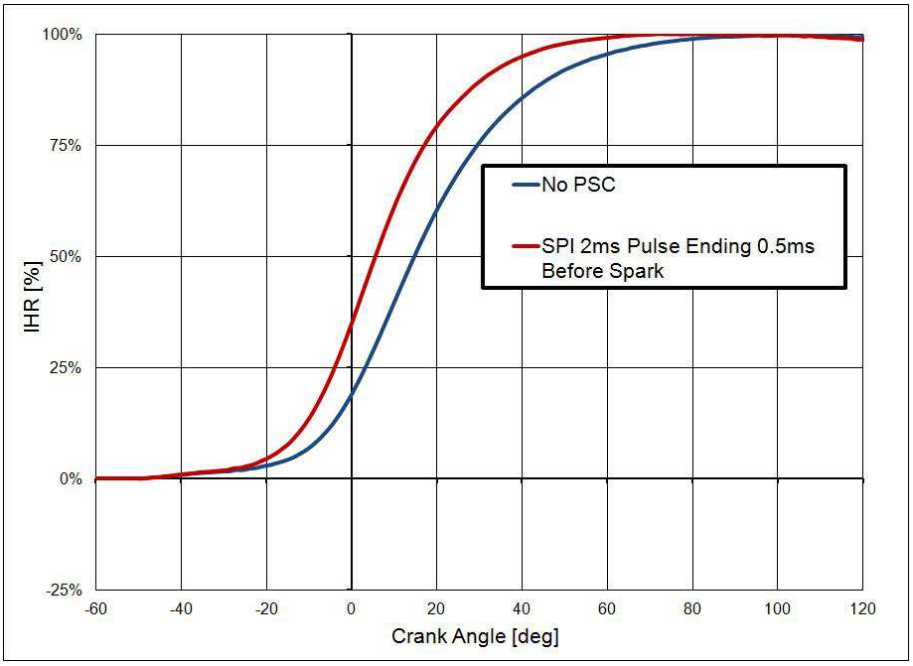

Figure 3.22: Integrated Heat Release vs. Crank Angle: 3000 rpm, λ = 1.65

As can be seen above, the use of a single-PSC-injection greatly increases the combustion speed and allows for a earlier start of combustion, over the no-PSC case.

To see why the double-PSC-injection cases are performing poorly at λ = 1.75, the IMEP vs. CA of maximum pressure are shown next.

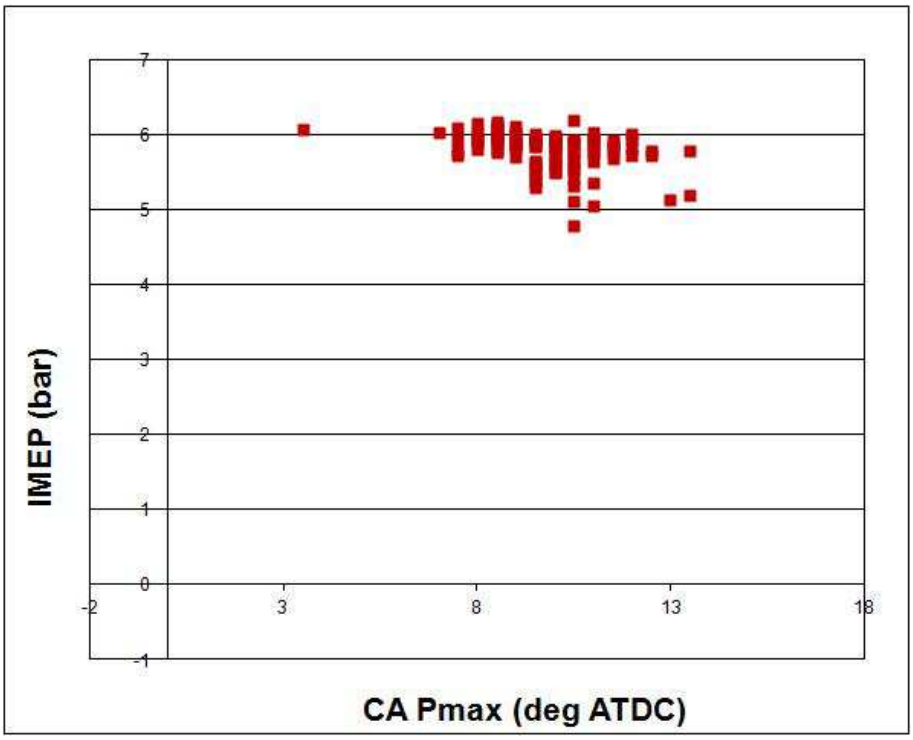

Figure 3.23: IMEP vs CA of Maximum Pressure for SPI: 3000 rpm, λ = 1.75

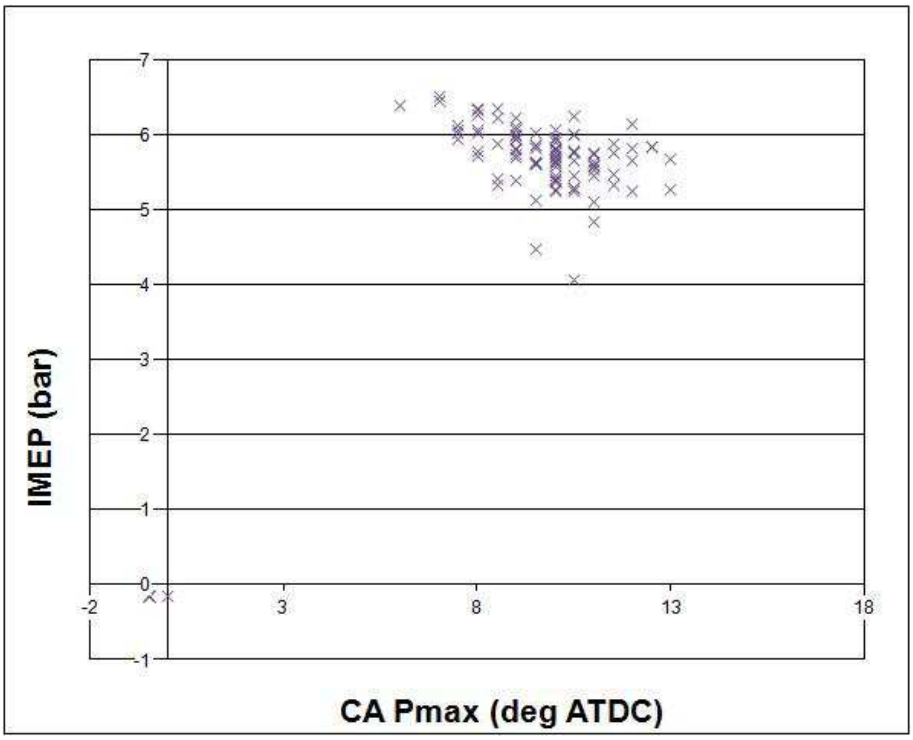

Figure 3.24: IMEP vs CA of Maximum Pressure for DPI 1ms Pulse Starting 1ms After Spark: 3000 rpm, λ = 1.75

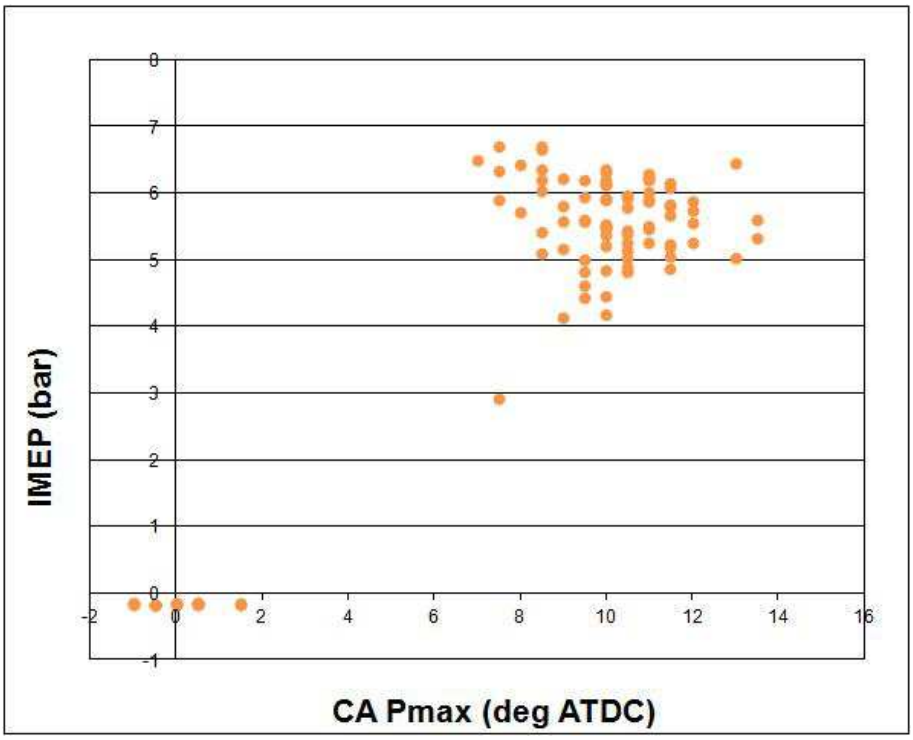

Figure 3.25: IMEP vs CA of Maximum Pressure for DPI 2ms Pulse Starting 0ms After Spark: 3000 rpm, λ = 1.75

From the graphs above it can be seen that all cases show good combustion but the two double-PSC-injection cases show cycles where there is no ignition of the air-fuel mixture at all (4% of cycles for the 1-ms-pulse starting 1-ms-after-spark case and 18% for the 2-ms-pulse starting 0-ms-after-spark). It is possible the second injection is, on occasion, creating an area around the spark plug electrode that is too rich to be ignited. Since there is little variation in COV of IMEP for all double-PSC-injection case with a 1-ms-pulse no matter what the timing, the same is true for all double-PSC-injection case with a 2-ms-pulse, this problem of no ignition does not seem to be related to the

timing but of the size of the second injection. When the second injection is larger, the area around the spark plug is more likely to be too rich for ignition.

The integrated heat release curves for the cases just presented are shown below to see if there are any differences in the timing and rate of combustion.

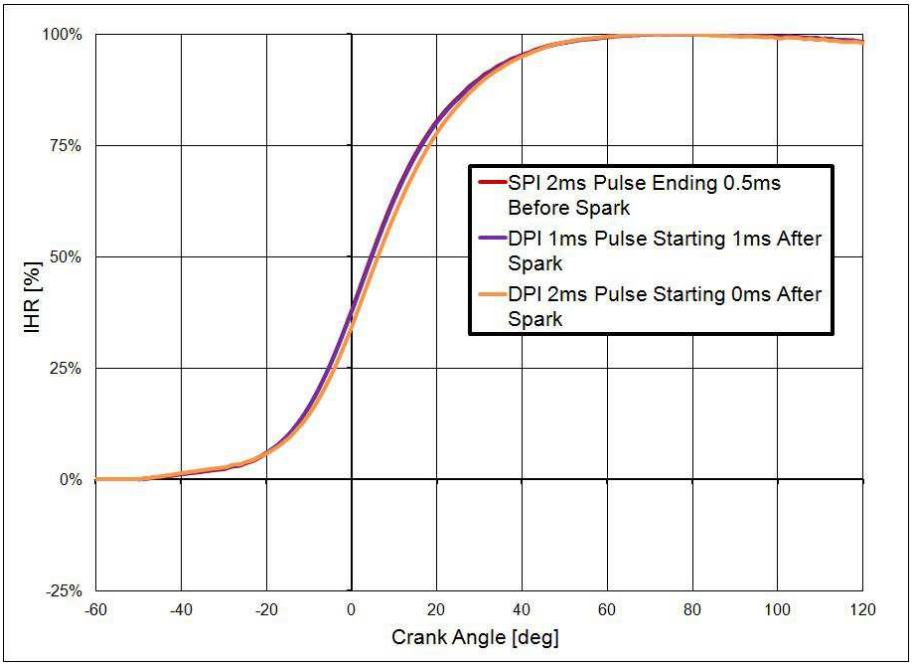

Figure 3.26: Integrated Heat Release vs. Crank Angle: 3000 rpm, λ = 1.75

At λ = 1.75, there is little variation between the heat release curves for the single and double-PSC-injection case. The single-PSC-injection case is barely visible in figure above because of it being almost identical to the double-PSC-injection case with a 1-ms-pulse starting 1-ms-after-spark. The double-PSC-injection case with a 2-ms-pulse starting 0-ms-after-spark is very close to being the same curve as well, with the

difference likely being due to the misfires discussed earlier.

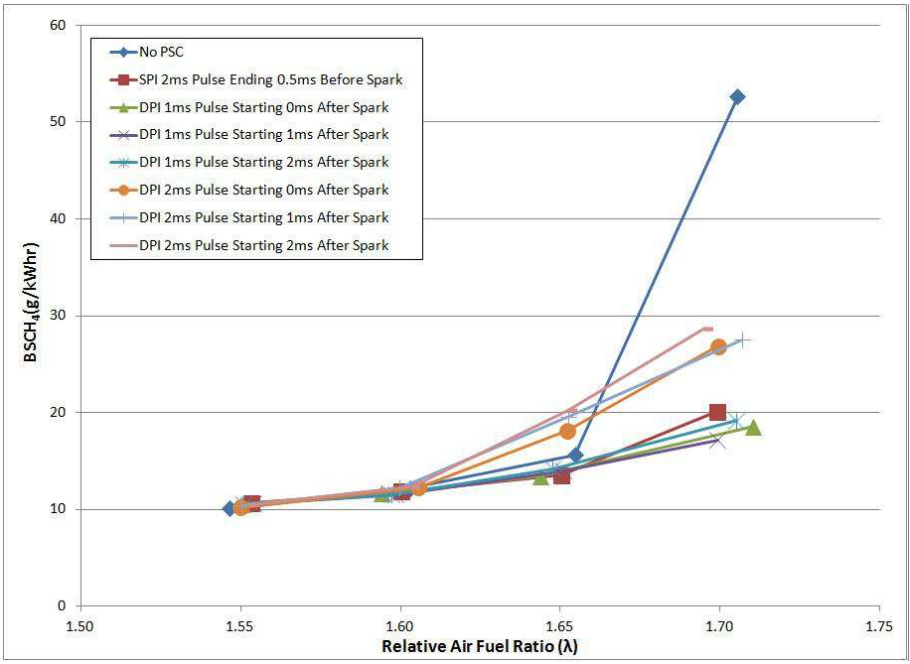

Figure 3.27: DPI - $BSCH_4$ vs.λ= 1.55-1.75 at 3000 rpm

The $BSCH_4$ graph shows improvement over the no-PSC case for the single-PSC-injection case and the 1 ms secondary injection-pulse-width for the double-PSC-injection cases for $\lambda \geq 1.65$, indicating improved combustion. The 2 ms secondary injection-pulse-width double-PSC-injection cases did not perform as well due to the higher PSC flow rate that resulted. This higher flow rate was not successful at improving combustion to compensate for the higher λ value of the bulk mixture for a given overall mixture λ value. No data is shown here for $\lambda > 1.70$ due to the limits of the total hydrocarbon (tHC) measuring equipment. The levels of tHC were too high

to be measured and since the tHC value is used in calculating the $BSCH_4$, no value for $BSCH_4$ could be calculated at higher λ values. This also true for $BSNO_X$ and the following graph does not show data for λ greater than 1.70 as a result.

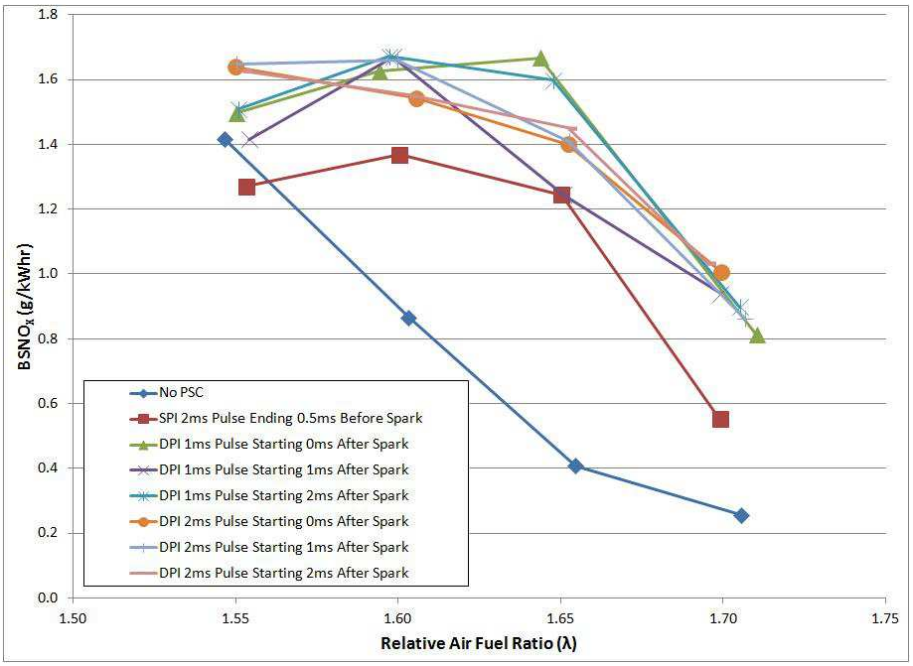

Figure 3.28: DPI - $BSNO_X$ vs.λ= 1.55-1.75 at 3000 rpm

The $BSNO_X$ graph is a bit messy just like the $BSNO_X$ graph for 1500 rpm is and for the same reasons. Again, the results of not perfectly picking the MBT spark timing can be seen. The graph does, however, trend down with increasing λ and cases with lower BSFC and COV of IMEP results have higher $BSNO_X$ values, both of which are expected.

The important results from the 3000 rpm test cases are as follows:

- Single-PSC-injection with an injection pulse of 2.5ms ending 0.5-ms-before-the-start-of-spark at λ = 1.65, improves BSFC by 4% and 7% over all double-PSC-injection cases with a secondary injection-pulse-width of 3 ms and the no-PSC case respectively. The same single-PSC-injection at λ = 1.70 improves BSFC by 30% over the no-PSC case; at λ = 1.75 it improves BSFC by 26% over all double-PSC-injection cases with a secondary injection-pulse-width of 3 ms. At $\lambda \leq 1.60$ there is no significant variation in BSFC between any of the cases run.

- Single-PSC-injection with an injection-pulse of 2.5 ms ending 0.5-ms-before-the-start-of-spark at λ = 1.65, reduces COV of IMEP by 4 and 12 % COV of IMEP over double-PSC-injection cases with a secondary injection-pulse-width of 3 ms and the no-PSC case respectively. The same single-PSC-injection reduces COV of IMEP at λ = 1.70, by 5, 16 and 24 % COV of IMEP over the double-PSC-injection cases with a secondary injection-pulse-width of 1 ms starting 2-ms-after-spark, double-PSC-injection cases with a secondary injection-pulse-width of 3 ms and the no-PSC case respectively. The same single-PSC-injection reduces COV of IMEP at λ = 1.75, by 17 and 40 % COV of IMEP over the double-PSC-injection cases with a secondary injection-pulse-width of 1 ms and double-PSC-injection cases with a secondary injection-pulse-width of 3 ms respectively. The same single-PSC-injection was also had a COV of IMEP of less than 10% at λ = 1.80 where all other cases produced engine operating condition so poor that data could not be taken.

- At λ = 1.65 there are no misfires for either the no-PSC or single-PSC-injection case but the single-PSC-injection case still reduces cycle to cycle variation in

IMEP and speeds up combustion showing that the use of PSC not only improves ignition but also combustion. At λ = 1.75 the double-PSC-injection cases do not perform as well as the single-PSC-injection case due to 4-18% of all cycles being misfires. This shows that the second injection in interfering with ignition.

- At λ = 1.65 the single-PSC-injection case with an injection pulse of 2.5 ms ending 0.5-ms-before-the-start-of-spark and double-PSC-injection cases with a secondary-injection-pulse of 1 ms, reduce $BSCH_4$ by 13% and 31% over the no-PSC case and the double-PSC-injection cases with a secondary injection-pulse-width of 3 ms, respectively. At λ = 1.70 the double-PSC-injection cases with a secondary-injection-pulse of 1 ms, on average, reduce $BSCH_4$ by 8%, 31% and 65% over the single-PSC-injection case, the double-PSC-injection cases with a secondary-injection-pulse-width of 3 ms and the no-PSC case, respectively.

- As is the case for the 1500 rpm tests, at 3000 rpm little can be said with regards $BSNO_X$ for the various cases run, due to the size of the uncertainty involved, except that $BSNO_X$ decreases with with increasing λ for all cases.

3.4 High λ Double-Injection Tests

After seeing an improvement in combustion from some of the double-PSC-injection cases over the single-PSC-injection case at 1500 rpm, more investigation was warranted. Additional tests were performed for λ greater than 1.70 in an attempt to see if the improvements were the result of double-PSC-injection or simply the result of having a higher PSC flow rate. Since only the double-PSC-injection cases with secondary

injection-pulse-widths of 1 ms resulted in improved combustion over the single-PSC-injection case, these are the only double-PSC-injection tests presented here. This was also the consideration for additional single-PSC-injection cases. The improved combustion seen in the double-PSC-injection cases could simply be from the increased PSC fuel flow. To see if this was the case, single-PSC-injection tests were performed with a 2.5-ms-injection-pulse-width ending 1.5-ms-before-spark. Note the injection timing did not change. The pulse lengths and timings for the data series labeled as DPI in the graph legends, refer to the secondary PSC injection.

All PSC tests were performed with a PSC pressure of 16 bar. All primary injections for double-PSC-injection cases had a 1.5-ms-pulse-width with the injection ending 1.5-ms-before-the-start-of-spark. As a reference the flowing table is presented to give estimations of the PSC injection flow rates and the percent of the total fuel flow rate that is from the PSC injection flow rate, for the PSC injection conditions used in the following tests.

Table 3.4: PSC Flow Rates at 1500 rpm, $\lambda \geq 1.70$

PSC Injection Type	Total PSC Injection Pulse Width (ms)	Total PSC Injection Flow Rate (g/hr)	Percent PSC of Total Fuel at λ = 1.75
Single-PSC-Injection 1.5 ms PSC Injection Pulse	1.5	13	2.0%
Single-PSC-Injection 2.5 ms PSC Injection Pulse	2.5	39	7.0%
Double-PSC-Injection 1 ms Secondary Injection Pulse	2.5	21	3.2%

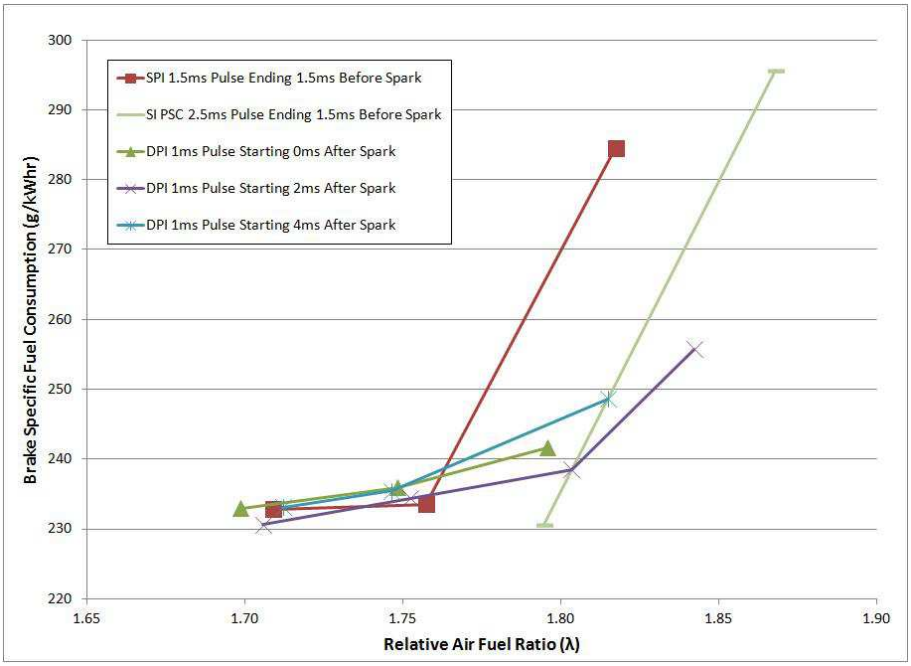

Figure 3.29: DPI - BSFC vs.λ= 1.70-1.85 at 1500 rpm

The BSFC graph shows an improvement in combustion for the higher flow rate single-PSC-injection over all other cases at λ = 1.80. It is difficult to tell if the higher flow rate single-PSC-injection case offers improved combustion over the other cases at λ = 1.85 due to the variation in actual λ values recorded. At higher λ values the percent error in controlling the fuel flow rate increased due to the decrease in fuel flow rate. Although, every attempt was made to gather data precisely at λ = 1.85 this was not what resulted and therefore no conclusions can be made for this λ value.

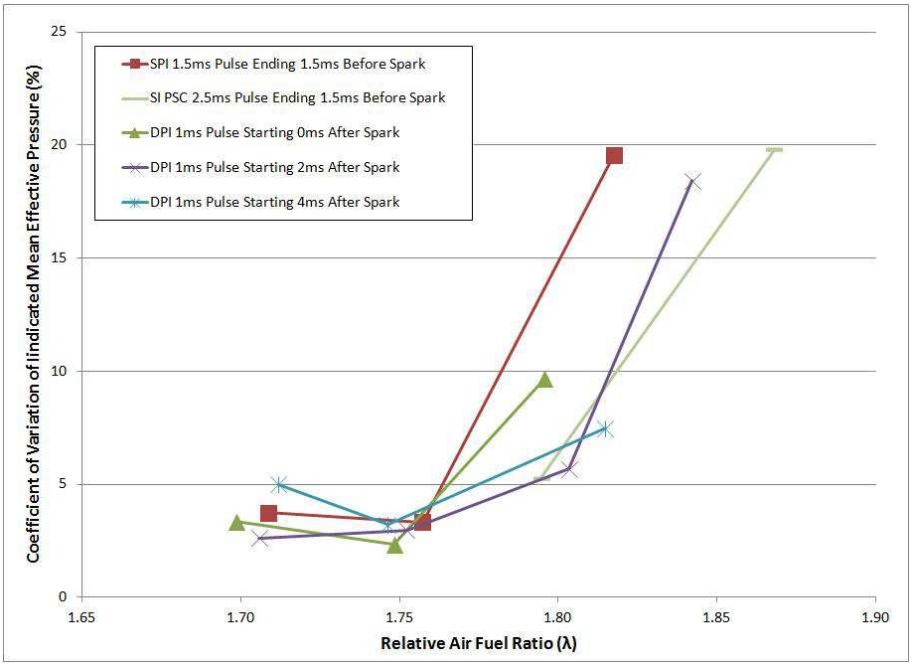

Figure 3.30: DPI - COV of IMEP vs.λ= 1.70-1.85 at 1500 rpm

Results similar to BSFC can be seen for COV of IMEP. The main difference is that it is not obvious as to whether the higher flow rate single-PSC-injection offers more reliable combustion over all other cases even at λ = 1.80. Data for each case at a λ value closer to 1.80 would be useful but additional tests were unable to be performed due to equipment failure.

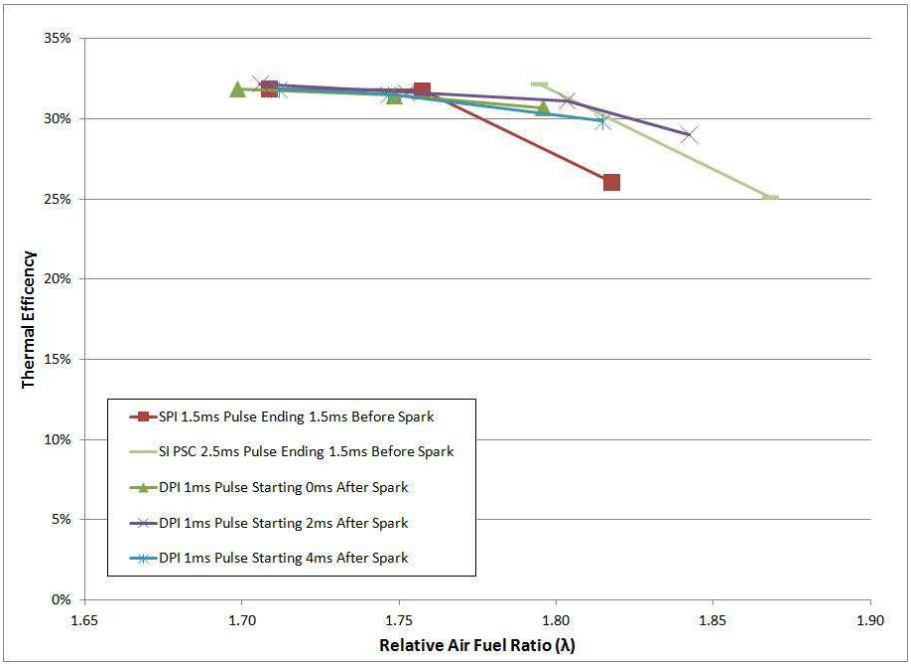

Figure 3.31: DPI - Thermal Efficiency vs.λ= 1.70-1.85 at 1500 rpm

The thermal efficiency graph is again only presented for reference.

Figure 3.32shows the IMEP and crank-angle of maximum pressure for each of the 100 cycles measured at a speed of 1500 rpm and λ = 1.8 using the SPI system.

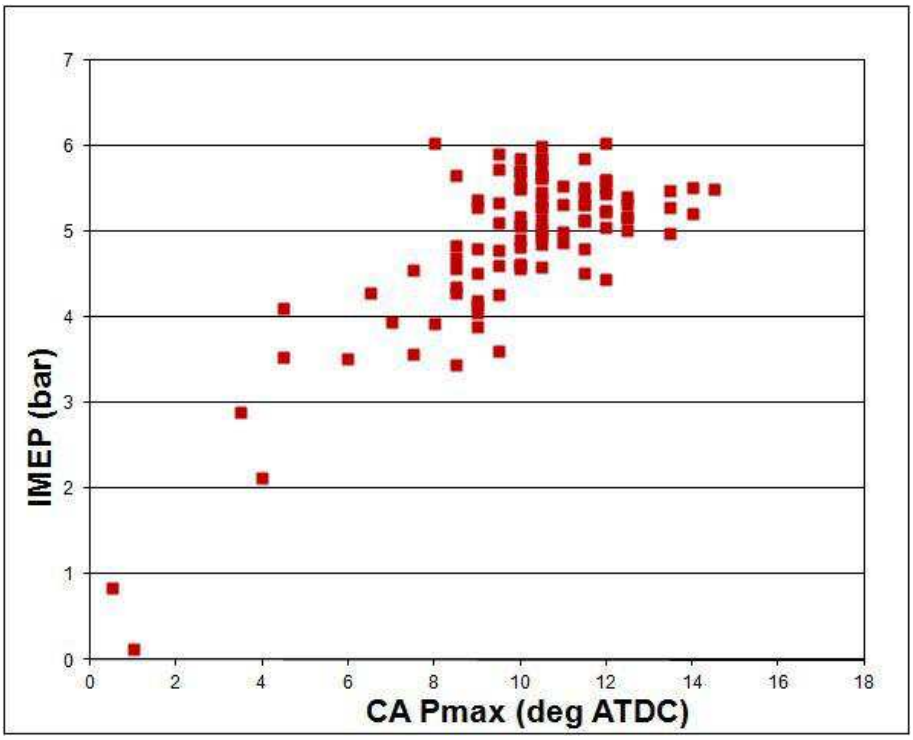

Figure 3.32: IMEP vs CA of Maximum Pressure for Low Flow SPI: 1500 rpm, λ = 1.80

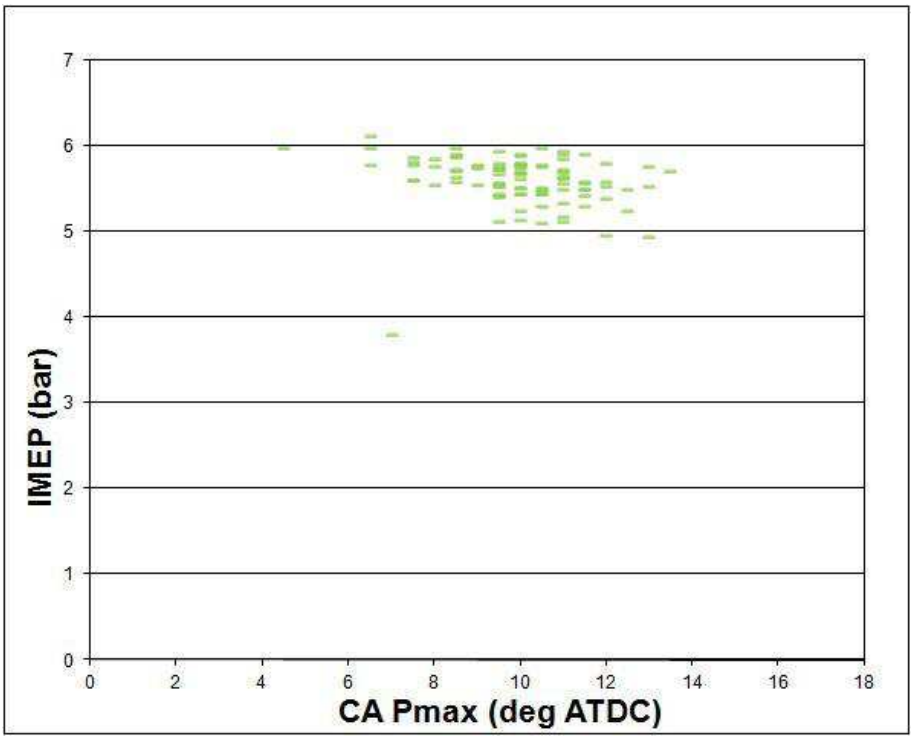

Figure 3.33: IMEP vs CA of Maximum Pressure for High Flow SPI: 1500 rpm, λ = 1.80

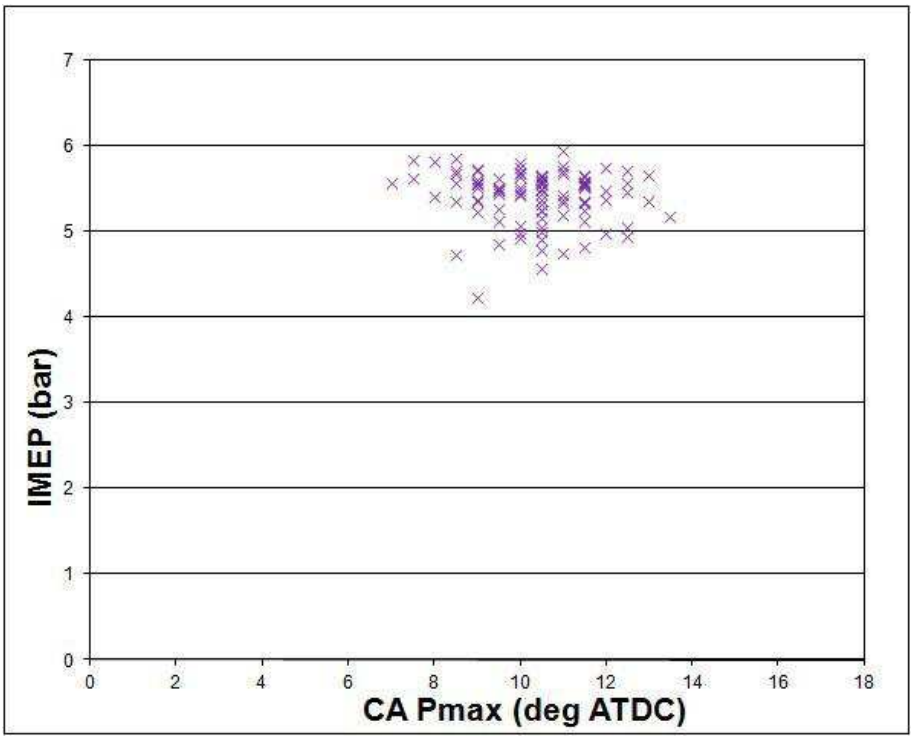

Figure 3.34: IMEP vs CA of Maximum Pressure for DPI 1ms Pulse Starting 2ms After Spark: 1500 rpm, λ = 1.80

For the low flow single-PSC-injection case (1.5-ms-pulse-ending-1.5-ms-before-spark) there are two near misfires and around 20 cycles with IMEP of less than 4.5 bar occurring before 10 degrees ATDC, compared to the high flow single-PSC-injection case (2.5-ms-pulse-ending-1.5-ms-before-spark) and double-PSC-injection (1-ms-secondary-pulse-starting-2-ms-after-spark) cases which only each have 1 cycle in the same region and neither of which has any misfires or near misfires. This shows that the low-flow single-PSC-injection case is failing in two ways; barely igniting the air-fuel mixture occasionally and frequently showing poor combustion when good ignition does occur.

The integrated heat release curves for the cases just presented are shown next to determine if there is any variation in combustion speed.

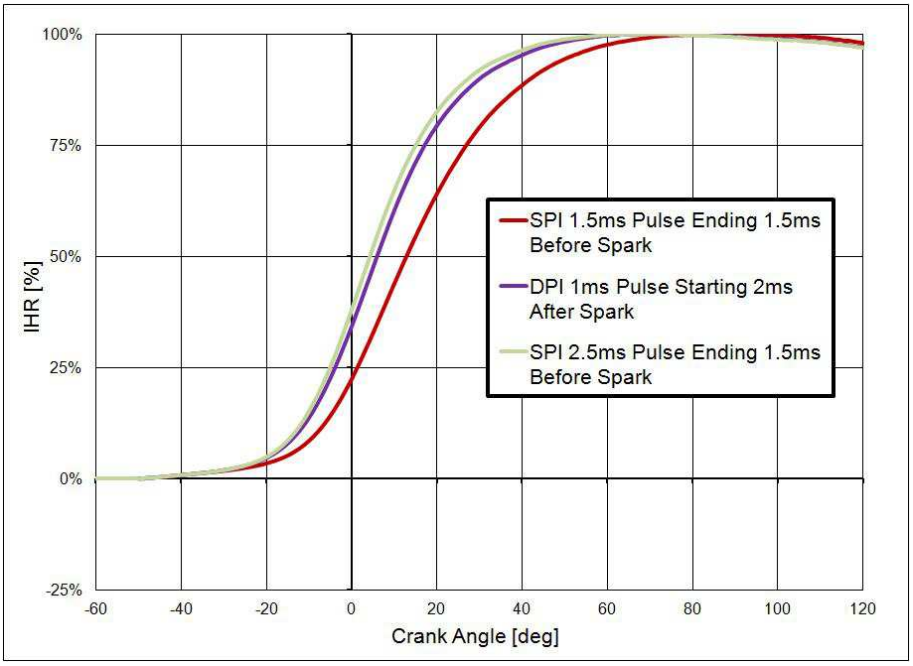

Figure 3.35: Integrated Heat Release vs. Crank Angle: 1500 rpm, λ = 1.80

The curves show that both the 2.5 ms pulse single-PSC-injection and the 1 ms pulse double-PSC-injection cases have increased combustion speeds over the no-PSC case, with the 2.5 ms pulse single-PSC-injection case being slightly faster than the 1 ms pulse double-PSC-injection case. This shows that larger PSC injections are needed for good combustion at high λ values.

The following graphs show difference between the high flow single-PSC-injection case and the same double-PSC-injection case at λ = 1.85, where both are still showing

high COV of IMEP.

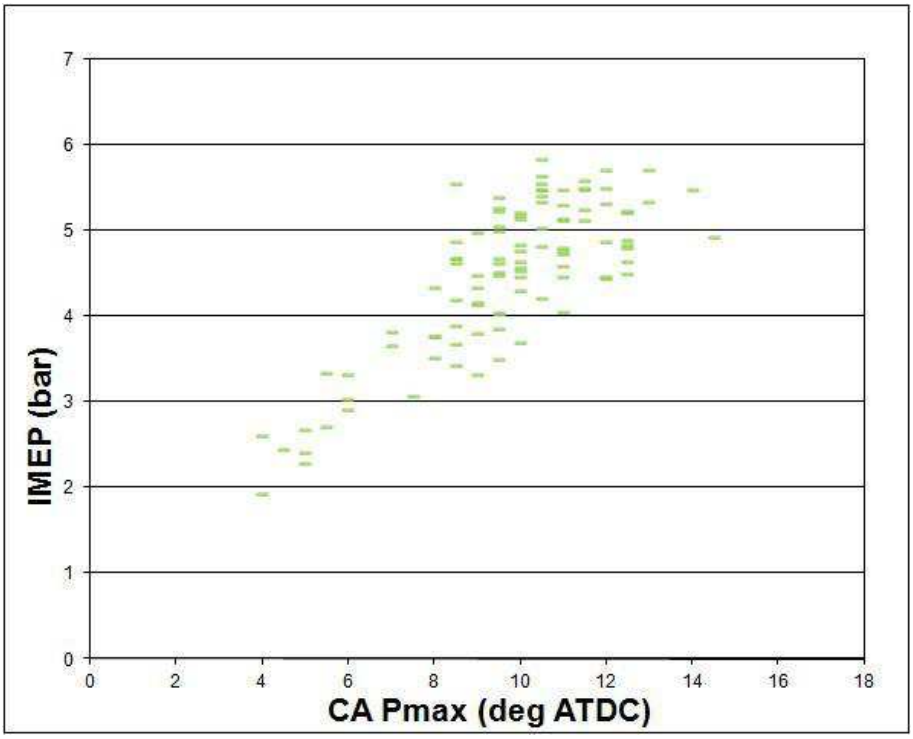

Figure 3.36: IMEP vs CA of Maximum Pressure for High Flow SPI: 1500 rpm, λ = 1.85

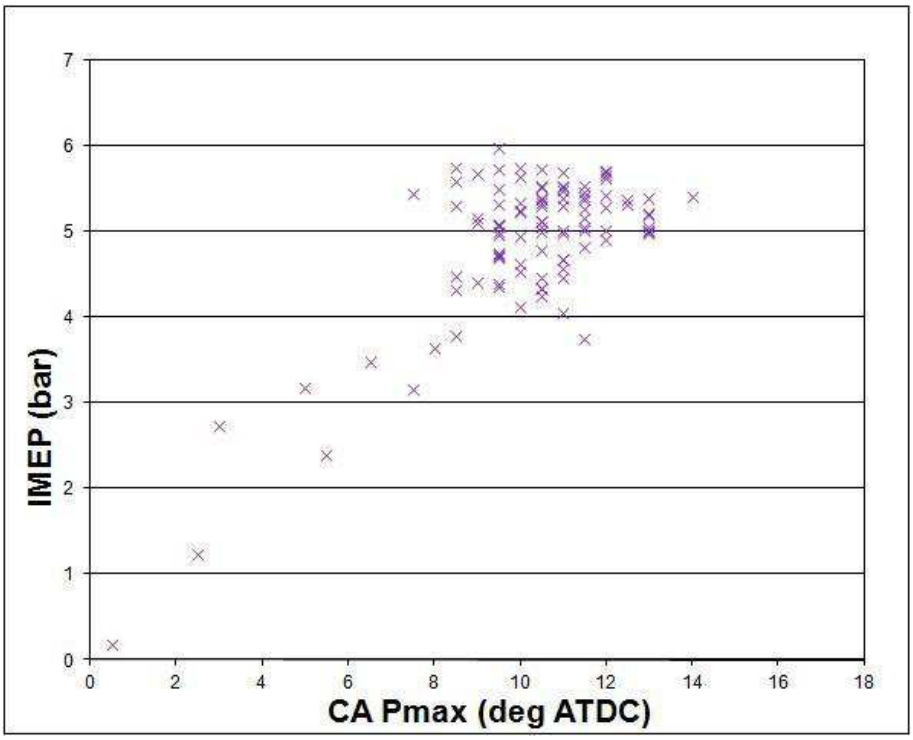

Figure 3.37: IMEP vs CA of Maximum Pressure for DPI 1ms Pulse Starting 2ms After Spark: 1500 rpm, λ = 1.85

Although the difference in COV of IMEP is small between the two cases, there is a noticeable different in the distribution of the points on the graphs. The single-injection case shows points spread more evenly over IMEP and crank angle, while the double-injection case shows 90% or more of it's points at higher IMEP and later crank angle, and a few points of poor ignition or very poor combustion. This may be the result of the primary injection for the double-injection case not being large enough or rich enough to properly ignite on some cycles, but on the majority of cycles when it does, the second injection is helpful in improving combustion of the bulk charge when compared to the

single-injection case.

The integrated heat release curves for the cases just presented are shown next to determine if there is any variation in combustion speed.

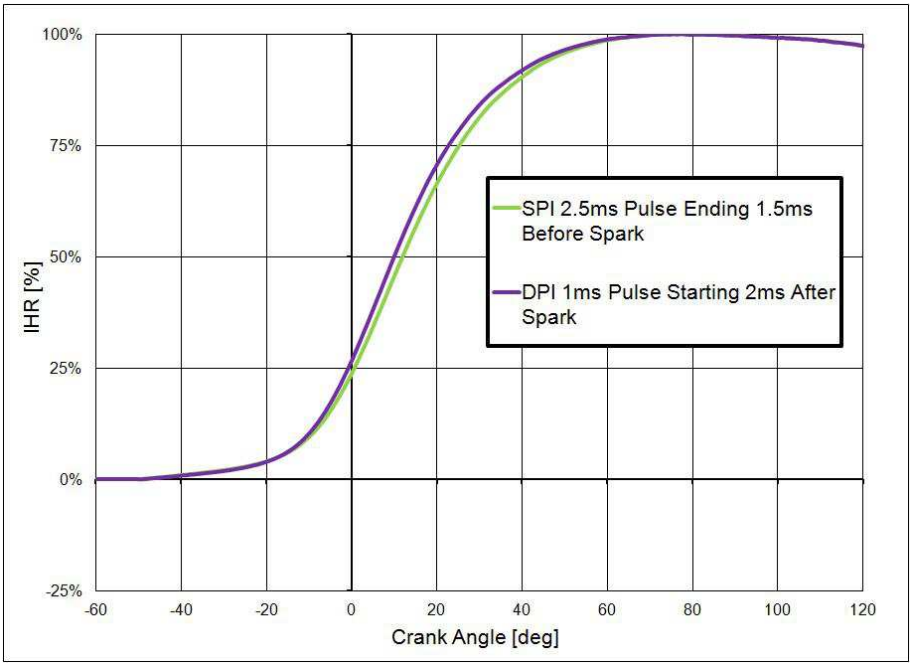

Figure 3.38: Integrated Heat Release vs. Crank Angle: 1500 rpm, λ = 1.85

Since both cases have the same ignition timing, it can be seen that the double-PSC-injection case increases the speed of combustion over the single-PSC-injection case despite the single-PSC-injection having a larger injection mass.

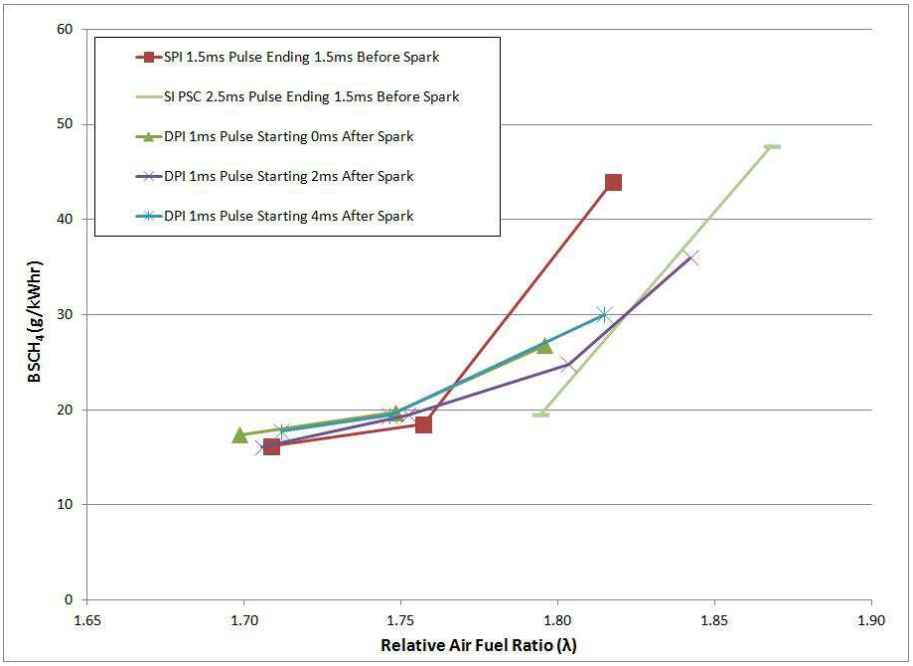

Figure 3.39: DPI - $BSCH_4$ vs.λ = 1.70-1.85 at 1500 rpm

The higher flow rate single-PSC-injection case offers improvements in $BSCH_4$ over all other cases. This, like the BSFC results, is a reflection of improved combustion.

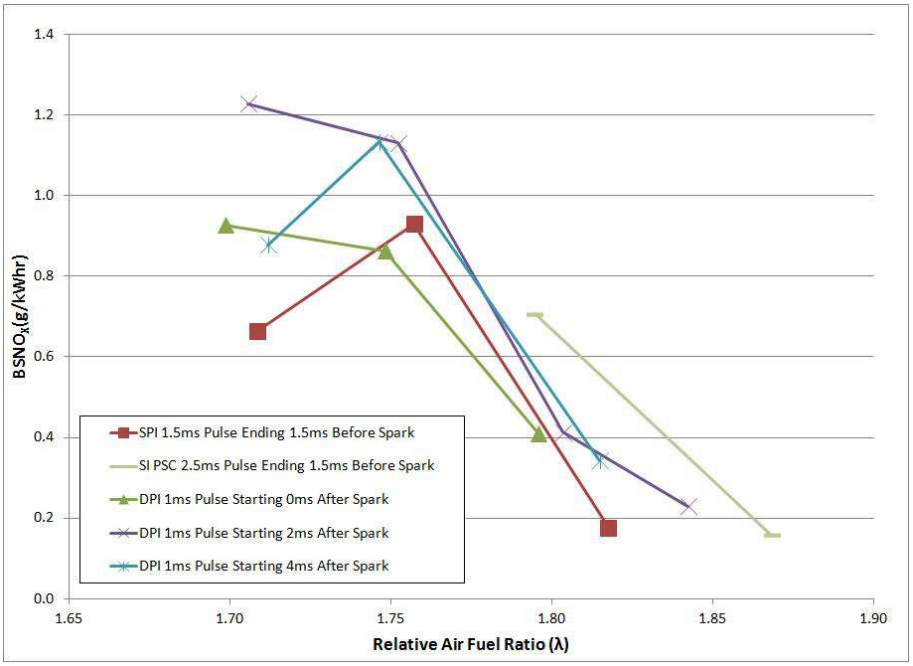

Figure 3.40: DPI - $BSNO_X$ vs.λ= 1.70-1.85 at 1500 rpm

The higher flow rate single-PSC-injection case has a higher value of $BSNO_X$ over all other cases at λ = 1.80 and 1.85. This is likely the result of improved combustion.

Overall, it appears that the higher flow rate single-PSC-injection case results in improved combustion but not necessarily more reliable combustion at λ = 1.80 compared to all other cases. At λ = 1.85, no conclusion as to which case performs best can be made. The important results from all the 1500 rpm test cases are as follows:

- Single-PSC-injection with an injection pulse of 1.5 ms ending 1.5-ms-before-the-start-of-spark improves BSFC by 1-2% at λ = 1.70 and 7-12% at λ = 1.75, over all double-PSC-injection cases with a secondary-injection-pulse-width of 3

ms. Single-PSC-injection with a injection pulse of 2.5 ms ending 1.5-ms-before-the-start-of-spark improves BSFC at λ = 1.80 by 4% and 8% over double-PSC-injection cases with a secondary injection-pulse-width of 1 ms starting 0 and 2 ms after the end of spark respectively. At $\lambda \leq 1.65$ there is no significant variation in BSFC between any of the cases run.

- Single-PSC-injection with an injection pulse of 1.5 ms ending 1.5-ms-before-the-start-of-spark reduces COV of IMEP by 8 and 12% COV of IMEP at λ = 1.70 over double-PSC-injection cases with a secondary injection-pulse-width of 3 ms starting 4 and 2 ms after the end of spark respectively. The same single-PSC-injection reduces COV of IMEP by 20 and 22 % COV of IMEP at λ = 1.75 over double-PSC-injection cases with a secondary injection-pulse-width of 3 ms starting 2 and 0 ms after the end of spark respectively. Single-PSC-injection with an injection pulse of 2.5 ms ending 1.5-ms-before-the-start-of-spark reduces COV of IMEP at λ = 1.80 by 4% COV of IMEP for the double-PSC-injection case with a secondary injection-pulse-width of 1 ms starting 0-ms-after-the-end-of-spark and by 14% COV of IMEP for the single-PSC-injection with an injection pulse of 1.5 ms ending 1.5-ms-before-the-start-of-spark. At $\lambda \leq 1.65$ there is no significant variation in COV of IMEP between any of the cases run.

- At λ = 1.85 the advantages of having a second injection are shown by 90% or more of double-PSC-injection cycles having a higher IMEP and later crank angle than the single-PSC-injection case, which shows a relatively even distribution of cycles over a larger range on IMEP and crank angle for maximum pressure and a few points of poor ignition or very poor combustion. The double-PSC-injection

case also shows a slight improvement in combustion speed over the single-PSC-injection case.

- All PSC cases have the same or higher $BSCH_4$ than the no-PSC case up until λ = 1.70 at which point the engine stops being able to operate without the use of PSC. Single-PSC-injection and double-PSC-injection with a secondary injection pulse of 1 ms reduces $BSCH_4$ by 32% and 24% at λ = 1.60 and at λ = 1.75 respectively over double-PSC-injection cases with a secondary injection-pulse-width of 3 ms. Single-PSC-injection with a injection pulse of 2.5 ms ending 1.5-ms-before-the-start-of-spark reduces $BSCH_4$ by 35% and 56% at λ = 1.80 over double-PSC-injection cases with a secondary injection-pulse-width of 3 ms and the single-PSC-injection with an injection pulse of 1.5 ms ending 1.5-ms-before-the-start-of-spark, respectively.

- Little can be said with regards $BSNO_X$ for the various cases run, due to the size of the uncertainty involved, except that $BSNO_X$ decreases with with increasing λ for all cases.

Chapter 4

Uncertainty Analysis

The graphs were presented in the Results section are quite full with data points due to the number of tests performed. With this taken into consideration, it is not practical to present the data uncertainty as error bars on the graphs. The data uncertainty is instead presented in table form in this section. The uncertainties for all data points are not provided, again, due to the number of data points. A representative sample of uncertainties, pertaining to 9 different tests, is presented here instead. These tests range in engine speed, λ, secondary PSC injection length and timing, as well as some that are only single-injection-PSC or no-PSC.

The uncertainties for λ, BSFC, $BSCH_4$ and $BSNO_X$ were calculated using the Root-Sum-Squared method. A description of this method is available in Appendix C. The following table gives a description of the test for which the uncertainties have been calculated, followed by two tables listing those uncertainties.

Table 4.1: Test Descriptions

Test #	Engine Speed (rpm)	λ	PSC Primary Injection		PSC Secondary Injection	
			Pulse Width (ms)	Timing Before Spark (ms)	Pulse Width (ms)	Timing After Spark (ms)
1	1000	1.30	N/A	N/A	N/A	N/A
2	1000	1.46	N/A	N/A	N/A	N/A
3	1000	1.62	N/A	N/A	N/A	N/A
4	1500	1.55	1.5	1.5	N/A	N/A
5	1500	1.65	1.5	1.5	1.0	2.0
6	1500	1.76	1.5	1.5	3.0	2.0
7	3000	1.55	2.0	0.5	2.0	2.0
8	3000	1.64	2.0	0.5	1.0	0.0
9	3000	1.70	2.0	0.5	N/A	N/A

Table 4.2: Calculated Uncertainties of λ and BSFC

Test #	λ			BSFC		
	Value	Uncertainty		Value (g/kW-hr)	Uncertainty (g/kW-hr)	(%)
			(%)			
1	1.30	0.11	9	228.77	1.24	0.5
2	1.46	0.14	10	226.85	1.25	0.5
3	1.62	0.17	10	233.03	1.31	0.6
4	1.55	0.10	6	225.63	0.91	0.4
5	1.65	0.11	7	229.66	0.95	0.4
6	1.76	0.12	7	265.46	1.19	0.4
7	1.55	0.05	3	241.21	0.71	0.3
8	1.64	0.06	4	245.77	0.76	0.3
9	1.70	0.06	4	264.83	0.91	0.3

Table 4.3: Calculated Uncertainties of Brake Specific Emissions

Test #	$BSCH_4$			$BSNO_X$		
	Value	Uncertainty		Value	Uncertainty	
	(g/kW-hr)	(g/kW-hr)	(%)	(g/kW-hr)	(g/kW-hr)	(%)
1	5.00	0.21	4	10.76	0.44	4
2	7.18	0.26	4	3.07	0.18	6
3	11.3	0.32	3	0.5	0.20	40
4	10.06	0.54	5	1.46	0.16	11
5	14.9	0.70	5	1.01	0.36	32
6	18.16	0.62	3	1.10	0.69	63
7	10.52	1.23	12	1.63	0.36	22
8	13.40	1.41	11	1.67	0.23	14
9	20.10	1.83	9	0.55	0.13	24

The calculated uncertainties show variations based on the test conditions as well as variations between variables. The uncertainty of λ varies between 3% and 10% with a higher percent uncertainty at higher λ values and lower engine speeds. At higher λ values the fuel flow rate is lower and since the uncertainty of λ is inversely proportional to the fuel flow rate squared, the uncertainty of λ increases faster than absolute value of λ. At higher engine speeds the fuel flow rate is higher for a given λ and due to the inverse relationship of the uncertainty to the fuel flow rate, the uncertainty is lower.

The uncertainty of the of the BSFC is quite low, ranging from 0.3% to 0.5%, due to the accuracy of the fuel flow meters and the brake torque meter, and due to these being the only measured uncertainties to be considered.

The uncertainty of the $BSCH_4$ varies between 3% and 12% and increases with increasing engine speed. At higher engine speeds the engine must burn more fuel per unit of torque at the same λ. Since the uncertainty of the $BSCH_4$is inversely proportional to the torque squared, this results in the uncertainty increasing faster than the absolute

value of $BSCH_4$.

For $BSNO_X$ the percent uncertainty becomes very large, up to 63%, at high λ values. This is due to the calculated value for $BSNO_X$ being very low resulting in the absolute uncertainty being a larger percent of the calculated $BSNO_X$. The uncertainty could be decreased by using a lower concentration calibration gas for the NO_X analyzer and/or using an analyzer that is designed to measure lower NO_X concentrations.

Chapter 5

Conclusions and Recommendations

5.1 Conclusions

No extension of the lean limit was found when using double-PSC-injection over single-PSC-injection at either 1500 or 3000 rpm. However, there are some other benefits of using a secondary injection that can be seen at 1500 rpm. When looking at the IMEP vs. Crank Angle for Maximum Pressure graphs, the use of a secondary injection shows consistently higher IMEP for the vast majority of engine cycles. There are still cases of poor ignition when compared to the high mass single-PSC-injection case, indicating that the if the primary injection for the double-PSC-injection case was increased slightly (still allowing for less fuel to be injected via PSC compared to the high mass single-PSC-injection case) the double-PSC-injection case may out perform the single-PSC-injection case due to the improvement in rate of combustion provided by the secondary injection.

Other possible double-PSC-injection cases were not tested due to time and equip-

ment constraints. PSC can be seen to improve ignition and combustion, as previously observed by Chan[12] and the secondary injection is able to improve combustion compared to the single-PSC-injection case. If the optimum primary and secondary injection conditions could be found, an improvement in engine performance over single-PSC-injection would likely be realized.

It was not possible to perform further tests at 1000 rpm. When attempting to run the 1000 rpm tests, the engine emissions would not stabilize. The emissions would climb and drop significantly once or twice during the time period that the data was to be gathered. The reason for the problem is unknown but it is believed to be due to the decreased exhaust temperature that occurs when running the engine at 1000 rpm. The preliminary 1000 rpm tests were performed on warmer days so the exhaust would not have lost as much heat while flowing to the emission analyzers. Further 1000 rpm testing was scheduled to be preformed to try and resolve this issue but equipment failure ended the investigation early.

The new PSC injection system has been successful at better controlling the PSC fuel flow due to the improved control of PSC injection duration and timing using the new gasoline direct injector in place of the previous solenoid valve. This has resulted in better engine performance. Reynolds[5] found that the old PSC system offered very little benefit when used at 3000 rpm where as the new system allows improved control of the PSC injection in both duration and timing, resulting in improved combustion at $\lambda \geq 1.65$. The lean limit of combustion, was able to be extended from λ = 1.65 to λ = 1.80 at 3000 rpm compared to no extension using the old PSC system. The best engine performance using PSC injection resulted when using a single-PSC-injection of 2.5 ms

ending 0.5 ms after spark at an injection pressure of 6 bar.

The lean limit was extended from λ = 1.65 to λ = 1.80 at 1500 rpm using PSC injection. A single-PSC-injection of 1.5 ms ending 1.5 ms after spark at an injection pressure of 16 bar gave the best engine performance results for $\lambda \leq 1.75$. At λ = 1.80 better engine performance was achieved by using a longer injection pulse. A single-PSC-injection of 2.5 ms ending 1.5 ms after spark at an injection pressure of 16 bar, gave the best engine performance results at this λ value. This indicates the importance of varying the PSC injection flow rate with respect to λ to ensure optimum engine performance.

5.2 Recommendations

More testing is required to definitively say whether or not there is any benefit to double-PSC-injection over single-PSC-injection. The first tests that should be considered involve separating the best case single-PSC-injection flow rate into two injections. This was considered after the unsuccessful results of extending the lean limit using additional PSC fuel flow rate for double-PSC-injection tests, but was not able to be tested due to equipment failure. It seems logical to try split injection tests since direct injection engines employ this method to improve combustion stability.

Since increasing the PSC flow rate at high λ values was able to extend the lean limit even further at 1500 rpm, this should be further investigated. Running tests at high λ values where the PSC injection-pulse-width, timing and pressure are varied from the optimum case for lower λ values, may allow for the lean limit of combustion to be

extended past λ = 1.80. It has already been shown to extend the lean limit from λ = 1.75 to λ = 1.80 at 1500 rpm.

Another consideration for future testing is varying the voltage provided to the PSC injector. Since the injector is capable of running at 150 V, vs. the 100 V provided for the testing performed so far, quicker opening and closing times may be achieved allowing for improved injection control. Injector characterizations tests have shown an opening and closing time of 10 ms at 100V, which is much slower than the 1 ms opening and closing time quoted by the manufacturer. Operating the injector with a 150 V power source may allow the opening and closing time provided by the manufacturer to be achieved.

Bibliography

[1] “The World Factbook 2011”, Washington, DC: Central Intelligence Agency, 2011.

[2] http://www.naturalgas.org/overview/background.asp, 2012.

[3] http://www.naturalgas.org/environment/naturalgas.asp, 2012.

[4] Heywood, J.B., “Internal Combustion Engine Fundamentals”, New York: McGraw-Hill, 1988.

[5] Reynolds, C., “Performance of a partially stratified-charge natural gas engine”, M.A.Sc. Thesis, Dept. of Mech. Eng., UBC, Vancouver, BC, 2002.

[6] Evans, R.L., “Control Method for Spark-Ignition Engines”, U.S. Patent 6032640, 2000.

[7] Evans, R. L., 1999a, “Lean-Burn Natural Gas Engines for High Efficiency and Low Emissions”, ICE-Vol. 32-2, Spring Technical Conference, ASME, 1999.

[8] Evans, R. L., “A Novel Stratified-Charge Engine Design for Low Emissions and High Efficiency”, Combustion Inst. Canadian Sect., 1999 Spring Technical Meeting, Paper No. 13, 1999.

[9] Evans, R.L., ed., “Automotive Engine Alternatives”, Plenum Press, 265 pp., 1987

[10] Logan, J., “Evaluation of a partially stratified charge insert in a natural gas engine”, M.A.Sc. Thesis, Dept. of Mech. Eng., UBC, Vancouver, BC, 2011.

[11] Gorby, D., “An evaluation of partially stratified charge ignition in a direct injection natural gas engine”, M.A.Sc. Thesis, Dept. of Mech. Eng., UBC, Vancouver, BC, 2007.

[12] Chan, E. C., “Spark Ignition of Partially Stratified Gaseous Fuel Air Mixtures”, Ph.D. Thesis, Dept. of Mech. Eng., UBC, Vancouver, BC, 2010.

[13] Arcoumanis, C., Hull, D., and Whitelaw, J., "An Approach to Charge Stratification in Lean-Burn, Spark- Ignition Engines," SAE Technical Paper 941878, 1994.

[14] Arcoumanis, C., Hull, D. R., and Whitelaw, J. H., “Optimizing local charge stratification in a lean-burn spark ignition engine”, Proceedings of the Institution of Mechanical Engineers, Part D: Journal of Automobile Engineering 211: 145, 1997

[15] Evans, R. L., Blaszczyk, J., “Fast-Burn Combustion Chamber Design for Natural Gas Engines”, J. Eng. Gas Turbines Power, Vol 120, Issue 1, pg. 232, Jan 1998.

[16] Evans, R.L., “Internal Combustion Engine Squish Jet Combustion Chamber”, U.S. Patent 4572123, 1986.

[17] Reynolds, C., and Evans, R.L., “Improving emissions and performance characteristics of lean burn natural gas engines through partial-stratification”, International Journal of Engine Research , vol. 5, No. 1, 2004.

[18] Iyer, R., Vaggar, M., Seetharam, T., and Channiwala, S., "Investigations on The Influence of Ignition Voltage, Higher Compression Ratio and Piston Crown Geometry on the Performance of Compressed Natural Gas Engines," SAE Technical Paper 2008-01-1762, doi:10.4271/2008-01-1762, 2008.

[19] Bell, S. R., Gupta, M., “Extension of the Lean Operating Limit for Natural Gas Fueling of a Spark Ignited Engine Using Hydrogen Blending”, Combust. Sci. and Tech., Vol. 123. pp.23-48, 1997.

[20] Ma, F., Wang, Y., Liu, H., Li, Y., Wang, J., Zhao, S., “Experimental study on thermal efficiency and emission characteristics of a lean burn hydrogen enriched natural gas engine”, International Journal of Hydrogen Energy, Volume 32, Issue 18, Pages 5067-5075, December 2007.

[21] Kastanis, E. J., “Jet Squish Motion in a Homogeneous-Charge Spark-Ignition Engine Fueled by Natural Gas”, M.A.Sc. Thesis, Dept. of Mech. Eng., UBC, Vancouver, BC, 2010.

Appendix A

Detailed Experimental Set-up

A.1 PSC Mechanical System

Compressed natural gas flows from the compressor at 4500 psi to the first of two regulator valves. Here the pressure is reduced to 1800 psi before traveling via 1/4” stainless steel tubing to a second regulator where the pressure is decreased to the desired PSC pressure (6 - 32 bar). The natural gas then flows through a mass flow meter (see Table C.1 in Appendix C for specifications) to the direct injector again via 1/4” stainless steel tubing. The natural gas continues on via 1/16” stainless steel tubing, through a check valve, to the PSC spark plug insert which delivers in to the combustion chamber. This system is identical to that used by Logan[10] with the exception that a direct injector was used to control the PSC fuel flow rate vs. the solenoid valve used by Logan.

A.1.1 PCS Spark Plug Insert

The insert was designed by Jean Logan[10] to test the effects of spray pattern on PSC. His results showed no distinct benefit of one spray pattern over another, therefore it the spray pattern was not deemed important for PSC testing. Due to the clogging of one of

the spray pattern insert, a different spray insert was used for the preliminary tests and the main tests. All of the main tests, single and double-injection, used the same spray pattern insert. An image of the PSC spark plug insert can be found as Figure 2.1 in Chapter 2.

A.1.2 Direct Injector

A Siemens gasoline piezo electric direct injector was used to control fuel flow for the stratified charge. The specifications for the injector when used as a gasoline direct injector are listed below.

Table A.1: Direct Injector Manufacturer's Specifications

Static Flow	> 35 g/s	Opening/Closing Time	> 0.15 ms
Maximum Flow	< 2 mg/stroke	System Pressure	50 - 200 bar
Injections per Cycle	up to 4	Minimum Open Time	1 ms

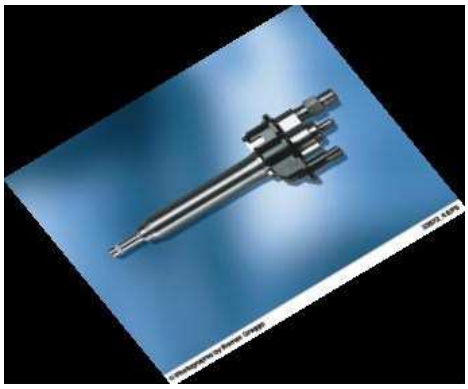

Figure A.1: Siemens Gasoline Piezo Electric Direct Injector

Test were run using a pressure transducer and computer software to determine the actual opening and closing times using natural gas as fuel and a 100 V signal. It was found that the injector took 10ms to fully open, which is greater than any injection durations used. It was also determined that there was a 0.5 ms delay between when the signal was sent to the injector driver compared to when the injector began to open.

A.2 PSC Electrical System

The electrical side of the PSC system starts at a desktop computer equipped with Lab-VIEW software. Here their are controls for PSC injection timing and duration; both of which are controlled in terms of crank angle degrees. The computer sends the timing and duration values to a timing card which sends a 5V digital signal to the injector driver at the appropriate time for the desired duration. The driver converts the 5V signal to a 100V signal, with an appropriate ramp up and ramp down, using a 100V power supply. The 100V signal opens injector and the injector closes when the signal ramps down.

The following electrical sections were written by Glenn Jolly, an electrical technician for the Mechanical Engineering department at the University of British Columbia, and were edited by this paper's author.

A.2.1 Engine Timing Overview

A four channel National Instruments NI 6604 PCI bus counter/timer card is used to generate the initial injection time relative to the position of the engine crankshaft. To do this the index pulse, which is generated from a rotary shaft encoder, is mechanically aligned to the TDC position of the engines piston. When the engine is operating the index pulse output signal produces exactly one pulse per revolution of the crank shaft. In one engine cycle two index pulses are generated, one pulse occurring just before the intake stroke, and one just before the power stroke begins. This index signal is then divided by two using an external flip flop circuit constructed using TTL integrated circuits. The divided signal will then produce a pulse aligned with the intake stroke . Each engine cycle will take 720 mechanical degrees to complete. The divided index pulse will then pulse only once to indicate a engine cycle is beginning and this is used as a reference to reset all four of the NI 6604 cards counters. The same rotary shaft encoder that produces the index pulse, also produces two pulse sequences identified as output Channels A an B which are 90 electrical degrees out of phase from each other. The encoder used is a 360 count per revolution counter, so it will produce 360 pulses on the A channel and 360 pulses on the B Channel, with only one mechanical revolution of its shaft. When the two encoder output channels are electrically combined, the electronics system is able to produce four electrical clock edges per degree of crank shaft rotation. In a 720 degree combustion cycle , this will produce exactly 2880 pulses or one pulse every 0.25 degrees of crankshaft rotation. This combined pulse sequence is then used to increment all four NI-6604 counters on the PCI card. One of the counters on the PCI card is used to control the initial injector opening time for the primary PSC

injection and another is used to do the same for the secondary PSC injection. A third is used for the spark timing and the last was not used for the experiments presented in this paper.

The counter logic blocks on the PCI card have some interesting features which allow the counters to be preloaded with a specific integer values controlled by the systems operator. One counter register holds a value representing the number of mechanical degrees the injector is to be held open. This counter integer value is equal to the mechanical degree angle divided by the base crank resolution of 0.25 degrees. When the timer count value is equal to the previously set value the counter output will assert a high logic level on its output indicating a start of injection request, the counter then decrements the pre-loaded value to zero before resetting the counter output signal to a logic low indicating the end of injection. The counter then automatically reloads the pre-set value well before the next cycle begins. The final injector control output signal is a pulse with the rising leading edge coincident with the user requested start of injector opening and the pulse width equal to the required injector hold open time. A falling edge of this signal indicates a injector close event. The injector control output signal is then connected to diode isolator box an then to the injector driver module. The diode isolator is used to control the injector for a two pulse injection.

A.2.2 Piezoelectric injector driver module

The piezoelectric injector driver module provides the electrical signal to the piezoelectric injector to cause it to open and allow fuel into the combustion chamber. The purpose of the module is to provide accurate fuel injection opening events and to hold

the injector open for the specified crank angle. In the system the piezoelectric injector initial time of opening is determined only by the engine crankshaft position. The closing time is determined by a user specified crank angle rotation which must occur after the initial opening.

General Overview

The injector timer controller uses a Microchip dsPic micro-controller to generate a pulse width modulation (PWM) control signal to a half bridge power amplifier, which is then electrically filtered and which will in turn will cause the injector to open. Additionally the micro-controller analog to digital converter is used to record the applied injector voltage signal and the injector current signal for examination on request. A quadrature input channel on the dsPic micro-controller is used to physically measure the crank angle at which the injector opens and the crank angle when the injector closes.

A system clock incremented by a 1 MHz clock can be used to measure the injector overall opening time. In the future these signals can be used to evaluate the injector performance and to provide fixed time offsets which more correctly indicate when the injector has physically opened after the open request was received. The PWM base clock frequency is 100 kHz.

The PWM output pulse width is generated from the PWM sub circuit within the micro-controller. The pulse width is controlled specifically by an internal dsPic PWM register value which is a 16 bit integer value. When the control register is assigned a value by the software the PWM sub circuit will maintain that pulse width until it is subsequently reprogrammed by the dsPic micro-controller. The output of the PWM circuit

is a complemented logic level signal and would not have enough current sourcing and sinking capacity to operate the injector directly so it is passed through an amplifier block to increase the current drive capability of the circuit.

PWM Amplifier

The PWM control signal is used to operate two output N-Channel MOSFET transistors which create a pulsing voltage drive signal of up to 200 Volts , The MOSFET peak current capability can be as high as 14 Amps without damage to the transistors. Only one output transistor is on at a time, either the high side driver or the low side driver. For example when the high side driver is turned off a delay time known as the dead band will prohibit the low driver from turning on for a few microseconds to protect the output transistors from damage. If both transistors were on a the same time a direct path from the power supply positive rail to the power supply negative exists which does not pass through the load and damage to the amplifier would result very quickly. When the high side MOSFET is turned on the power supply positive supply rail is connected directly to the output filter. When the low side MOSFET driver is turned on the output filter input is connected directly to the negative DC rail power. These output pulses have a fast rise time of 2 ms and rise to a peak output voltage of typically 100 VDC. The application of voltage to the filter will either add or remove charge from the Injector.

PWM Amplifier Output Filter

The MOSFET output pulse voltage is applied to the resistor of a inductive resistive filter (L/R Filter) . The series resistor in the filter is used to lower the L/R time constant of the circuit and reduce electrical distortion of the output circuit currents. Additionally a resistor across the inductor can be used to lower the Q or quality of the filter to reduce ringing at or near the leading edge of the PWM signal. When a high voltage is applied to the filter from the upper half bridge MOSFET driver, during the logic high PWM signal On time, the current in the filters series circuit begins to rise exponentially toward the maximum current. It is, however, only on for a short period of time before the PWM signal turns off again. The peak value that the current can rise to is determined by the piezoelectric load characteristics and the applied pulse width. The longer the pulse width the higher the current becomes eventually it would only be limited by the series resistance and the resistance of the injector but the drive signal is turned off before this occurs.

When the current is flowing through the series inductor and resistor it is also passing into the injector and electrical charge is being stored in the injector capacitance. The rate of current rise is limited by the inductance of the filter and the small resistance in series with it. During the switch on time electric charge is passed to the injector piezo stack negative terminal as a flow of electrons. The charge on the piezo stack causes the injector stack to expand and the injector to open. The rate at which it opens and how far it opens can be determined by the applied waveform pulse width and the peak voltage applied to the injector driver circuit power supply rails.

The capacitance of the injector is also a factor in how much charge must be trans-

ferred to the injector to cause it to open. The capacitance of the injector is controlled by the physical size of the metalized surface on each side of the piezoelectric material in the injector, the dielectric constant of the piezoelectric material used to construct the injector and the thickness of the piezoelectric material and the number of layers the injector actuator is constructed from. Other time varying parameters of the piezo material and the mechanical time constant of the actuator, as well as applied mechanical loads on the actuator, also affect the capacitance of the actuator assembly.

The voltage which is produced on the injectors electrical terminals is a function of the electrical charge transferred to the injector which is controlled by the current flowing to the injector and the time for which the current flows. Since the shape and of the current applied is generally an exponential shape, an integration must be performed over the time the current flows in order to measure the amount of electrical charge transferred to the injector piezo stack. The voltage measured across the piezo injector terminals is a function of all of these individual parameters.

In addition, the piezo injector responds to the physical force placed on it from the cylinder pressure so small variations of the voltage can be attributed to the physical cylinder pressure but our experiments did not attempt to determine these components. Substantial work would be required to model the injector drive waveform and subtract it from the measured injector voltage to leave only the engine induced effects in the resulting signal but such feedback is possible.

The inductor used in the output filter is 330 mH. The inductor is rated at a peak current of 14 A. At currents higher than this limit the magnetic field in the inductor core saturates and the current rises very quickly limited only by the series resistance

of the inductor and its series filter resistor. So care is taken that the filter time constant (L/R) is long enough it does not saturate the inductor core during the on pulse from the controller. The high frequency 100kHz PWM signal from the controller is not passed through the filter due to the cutoff frequency of the filter. There is a limited time for the current to build up during the short 10 ms time period the output transistors are turned on, however, the low frequency content 200 ms ramps will pass through the filter and as such only the envelope of the signal is visible as a voltage signal on the output side of the filter, at the injector terminals. This is essentially just a rectangular pulse with 200 ms edge times. This lower frequency signal will cause current to flow to the injector and charge is transferred to the injector.

Injector Micro-controller Controller Specifications

A Microchip dsPic Micro-controller is programmed to monitor the injector opening request line from the timing circuit electronics previously described and generate a PWM signal which is sent to a power amplifier to operate the injector. The processor used is a dspic30F6011A with the following partial list of features:

- 24 bit instruction width
- 16 bit data path width
- 80 external pins
- 144K of flash program Memory
- 8192 static RAM
- 4096 EEPROM

- 5 internal 16 bit timers
- 8 input capture pins
- 8 std PWM signal outputs
- 8 Motor Control PWM outputs
- 1 ADC
- 1 quadrature Encoder
- 2 UARTS
- 2 SPI
- 1 IIC
- 2 CAN bus ports

This micro-controller is installed on a Microchip motor controller demonstration board (MC1). The Oscillator on the demonstration board is a 7.3728 MHz crystal an internal phase lock loop (PLL) is operated in a multiply by 16 mode which is then divided by 4 to get the following clocks internally in the micro-controller.

- Fpll = 117.964800 MHz is the phase locked loop operating frequency
- FCY = 29.491200 MHz is the main processor clock frequency
- PWM base frequency is approximately 100KHz

Injector Signal Edge Characteristics

When the rising edge of the injector request line occurs, the PWM circuit is passed the first pulse width value to maintain from an internal turn-on array of 20 elements. This is the first element of a twenty element array which describes the shape of the leading edge of the injector pulse. The PWM rate of 100 kHz produces a update rate of 10 ms , and every 10 ms the PWM sub circuit interrupts the microprocessor to produce an interrupt which is used to update the PWM table with the next element from the array. The effect is to produce a set of twenty steps of increasing pulse width creating a transition that takes 200 ms to complete and produces a leading edge slope on the injector waveform. During this 200 ms the injector voltage transitions from 0 VDC to 100 VDC. The injector hold open signal is a constant signal at the 90% duty cycle producing a constant voltage to the injector of about 100 V. When the timing controllers output pulse falls, it signifies the end of the injector pulse and the negative edge of the timing controller signal causes an interrupt which loads the first element of the trailing edge array. This array decreases the width of the PWM sub circuit in 20 steps back to a short pulse width. The leading and trailing edge slope arrays can be edited separately to adjust the desired voltage or current waveforms.

The leading and trailing edge transitions lower the high frequency content of the injector pulse and minimize noise and current peaks to the injector. In addition the injector can be damaged by high current signals as they do not allow sufficient time for charge to be distributed through the piezo stack and mechanical cracking of the piezo stack structure can occur quite quickly. Once damaged the stack cannot be repaired.

A.3 PSC System Timing Characteristics

The injector was run with an oscilloscope connected to the input and output sides of the driver to ensure proper operation of the driver. The oscilloscope traces showed a 0.5 ms delay between the input and output signals. With this electrical delay and the 0.5 ms mechanical delay determined by the injector characterization tests, the PSC injections can be considered to have finished 1 ms later than the injection timing inputted into the LabVIEW program.

A.4 Fuel

Natural gas supplied by Terasen Gas lines is used to fuel the engine both for the homogeneous and stratified charges. The homogeneous charge uses gas at the line pressure of approximately 50 psi while the stratified charge uses gas that has been compressed then adjusted down to the desired pressure using the double regulator system mentioned earlier. The composition of the natural gas on Oct 3rd, 2011 is shown on the following page.

Table A.2: Westport Natural Gas Composition Oct 3rd 2011

	Air at STP
P, Pa	101325.0
M	28.962
R	8314.2
T, K	288.0
Y, kg/m^3	1.226

Avg. Molec. Wt.	16.390			
NG HHV (MJ/kg)	53.77	1001.8 Btu/ft^3	37.30	MJ/m^3
NG LHV (MJ/kg)	48.51	903.8 Btu/ft^3	33.65	MJ/m^3
NG LHV/HHV	0.902			
Rel. Density	0.566			
NG Density (kg/m^3)	0.694			
H/C ratio	3.899			
Wobbe Index, MJ/m^3	49.576			

Gas component	Molec. Wt.	HHV Btu/lb	HHV kJ/kg	LHV Btu/lb	LHV kJ/kg	LHV/HHV	Mol% from Micro GC	Mol%	Mass%	Rel. HHV kJ/kg	Rel. LHV kJ/kg	Mol% H	Mol% C
n-Butane (C_4H_{10})	58.118	21308.0	49515.29	19680.0	45732.16	0.924	0.098	0.098%	0.0035	171.40	158.30	0.0098	0.0039
i-Butane (C_4H_{10})	58.118	21257.0	49396.77	19629.0	45613.65	0.923	0.081	0.081%	0.0029	142.08	131.20	0.0081	0.0032
i-Pentane (C_5H_{12})	72.144	21052.0	48920.40	19478.0	45262.75	0.925	0.024	0.024%	0.0011	51.50	47.65	0.0029	0.0012
n-Pentane (C_5H_{12})	72.144	21091.0	49011.02	19517.0	45353.38	0.925	0.019	0.019%	0.0008	41.03	37.97	0.0023	0.0010
Hexane (C_6H_{14})	86.180	20783.0	48295.30	19232.0	44691.10	0.925	0.006	0.006%	0.0003	16.49	15.26	0.0009	0.0004
Heptane (C_7H_{16})	100.200	20681.0	48058.27	19345.6	44955.00	0.935	0.000	0.000%	0.0000	0.00	0.00	0.0000	0.0000
Octane (C_8H_{18})	114.230	20604.0	47879.34	19228.1	44682.00	0.933	0.000	0.000%	0.0000	0.00	0.00	0.0000	0.0000
Nitrogen (N_2)	28.016	0.0	0.0	0.0	0.0	0.0	0.517	0.517%	0.0088	0.00	0.0	0.0000	0.0000
Methane (CH_4)	16.041	23879.0	55489.75	21520.0	50007.93	0.901	93.394	93.394%	0.9140	50720.21	45709.57	3.7357	0.9339
Carbon Dioxide (CO_2)	44.011	0.0	0.0	0.0	0.0	0.0	0.651	0.651%	0.0175	0.00	0.0	0.0000	0.0065
Ethane (C_2H_6)	30.067	22320.0	51866.96	20432.0	47479.65	0.915	2.120	2.120%	0.0389	2016.71	1846.12	0.1272	0.0424
Propane (C_3H_8)	44.092	21661.0	50335.58	19944.0	46345.64	0.921	0.453	0.453%	0.0122	612.76	564.19	0.0362	0.0136
								0.9736	1.0000	53772.18	48510.26	3.9231	1.0061

Appendix B

Calculated Values

The following describes the how the values presented in the Section 3 were calculated. All formulas where taken from Haywood[4].

B.1 Relative Air-Fuel Ratio (λ)

The relative air-fuel ratio is defined as:

$$\lambda = \frac{\dot{m}_{air,dry}}{\dot{m}_{fuel}} \cdot \frac{1}{(A/F)_{stioch}} \tag{B.1.1}$$

where $\dot{m}_{air,dry}$is the mass flow rate of air entering the engine, $\dot{m}_{fuel}$is the mass flow rate of the fuel and $(A/F)_{stioch}$is the stoichiometic air fuel ratio. For stoichiometic conditions λ = 1. For lean (excess air) conditions λ > 1. For rich (excess fuel) conditions λ < 1.

B.2 Brake Specific Fuel Consumption (BSFC)

The BSFC is defined as:

$$BSFC = \frac{\dot{m}_{fuel} \cdot 1000 \cdot 60}{T_B \cdot N \cdot 2 \cdot \pi} \tag{B.2.1}$$

where $\dot{m}_{fuel}$ is the mass flow rate of fuel in g/hr, T_B is the engine brake torque in Nm and N is the engine speed in rpm. This gives the BSFC in units of g/kWhr.

B.3 Coefficient of Variation of Indicated Mean Effective Pressure (COV of IMEP)

The COV of IMEP is given as a percentage and is defined as:

$$COVofIMEP = \frac{\sigma_{IMEP}}{IMEP_{avg}} \cdot 100 \tag{B.3.1}$$

where $\sigma_{IMEP}$is the standard deviation of the indicated mean effective pressure and is defin1ed as:

$$\sigma_{IMEP} = \sqrt{\frac{1}{100} \cdot \left[(x_1 - IMEP_{avg})^2 + (x_2 - IMEP_{avg})^2 + ... + (x_{100} - IMEP_{avg})^2 \right]} \tag{B.3.2}$$

and $IMEP_{avg}$ is the average gross indicated mean effective pressure (IMEP), where the IMEP is defined as

$$IMEP = \frac{\oint PdV}{V_S} \tag{B.3.3}$$

where $\oint PdV$ is the area contained within the pressure-volume curve for the cycle (the work done by the engine) and V_S is the cylinder swept volume. For calculating σ_{IMEP}, the IMEP for 100 consecutive engine cycles is taken, where $x_1$is the first point, $x_2$is the second point, etc.

B.4 Thermal Efficiency

The thermal efficiency is defined as:

$$\eta_t = \frac{W_c}{W_p} = \frac{W_c}{\eta_c \cdot m_f \cdot Q_{HV}} \tag{B.4.1}$$

where $W_c$is the work done by the engine in one cycle, W_p is the energy released during combustion (the maximum work possible if the all the energy was converted into mechanical energy),η_c is the combustion efficiency (proportion of energy stored in the fuel that is released during combustion), m_f is the mass of fuel supplied for one engine cycle and Q_{HV} is the energy stored in the fuel per unit mass. The result is that the thermal efficiency gives the proportion of energy that is converted into mechanical energy of the total energy released during one engine cycle.

B.5 Brake Specific Methane ($BSCH_4$)

The $BSCH_4$is calculated using the mass flow of methane in the exhaust gas and the brake power as follows:

$$BSCH_4 = \frac{\dot{m}_{CH_4} \cdot 60}{T_B \cdot N \cdot 2 \cdot \pi} \tag{B.5.1}$$

where $\dot{m}_{CH_4}$ is the mass flow of methane in the exhaust in gas g/hr, T_B is the brake torque in Nm and N is the engine speed in rpm. The numbers 2 and 60 and the term π are used to covert the units so that the resulting value for $BSCH_4$ is in g/kWhr.

B.6 Brake Specific Nitrogen Oxides($BSNO_X$)

The $BSNO_X$is calculated using the mass flow of nitrogen oxides in the exhaust gas and the brake power as follows:

$$BSCH_4 = \frac{\dot{m}_{NO_X} \cdot 60}{T_B \cdot N \cdot 2 \cdot \pi} \tag{B.6.1}$$

where $\dot{m}_{NO_X}$ is the mass flow of nitrogen oxides in the exhaust gas in g/hr, T_B is the brake torque in Nm and N is the engine speed in rpm. The numbers 2 and 60 and the term π are used to covert the units so that the resulting value for $BSNO_X$ is in g/kWhr.

Appendix C

Detailed Uncertainty Analysis

C.1 Engine and Emissions Instrumentation Uncertainties

Below is a table of the accuracies of the instruments used for the experiments. These values were used in the uncertainty analysis that appears in the 4 chapter.

Table C.1: Engine and Emissions Instrumentation Specifications

Instrument	Make	Model	Range	Accuracy
Crankshaft Position	US Digital	H1-360	360ºCA	±1º
Brake Torque	BLH Electronics		0-48 Nm	±0.1% FS
Optical Shaft				±5 rpm
Universal Exhaust Gas Oxygen	Bosch	LSU4.2	0.7-2.0λ	±0.05λ
LFE Delta Pressure	Omega	PX653	0-10"H_2O	±0.25% FS
Intake Manifold Pressure	PCB Piezotronics	1501B01FB3BARA	0-3 bar	±0.25% FS
Intake Manifold Temperature		K Type	-200-1200ºC	±1.5ºC
Ambient Pressure	PCB Piezotronics	1501B01FB3BARA	0-3 bar	±0.25% FS
Relative Humidity	Ohmic Instruments	HC-610	0-100% RH	±2.0% FS
Exhaust Temperature		K Type	-200-1200ºC	±1.5ºC
Cylinder Pressure	AVL	QC33C	0-200 bar	±0.18% FS
Oil Temperature		K Type	-200-1200ºC	±1.5ºC
Oil Pressure	AutoTran	250G100P 3 N	0-100 psig	±1.0% FS
Coolant Temperature		K Type	-200-1200ºC	±1.5ºC
Fuel Mass Flow (Homogeneous Charge)	MKS	1559A-100C-SV	0-100 slm	±1.0% FS
Fuel Mass Flow (Stratified Charge)	MKS	179A-24C-S3BM	0-20 slm	±1.0% FS
Non-dispersive Infrared (CO_2)	ABB	Uras 14	0-2600 ppm	<1% FS
Chemiluminescence (NO_X)	AVL	CLD 4000	0-4300 ppm	<1% FS
Flame Ionization (CH_4)	Pierburg	FID 4000		<1% FS
Paramagnetic Oxygen (O_2)	ABB	Magnos 106	0-22%	<1% FS

C.2 Root-Sum-Squared Uncertainty Calculations

The Root-Sum-Squared method states that given a final, measured result, R, that is a function of measured quantities, x_i, where i ranges from 1 to n,

$$R = f(x_1, x_2, ..., x_n) \tag{C.2.1}$$

the uncertainty of R is calculated as

$$u_R = \sqrt{\left(\frac{\partial R}{\partial x_1} \cdot u_{x_1}\right)^2 + \left(\frac{\partial R}{\partial x_2} \cdot u_{x_2}\right)^2 + ... + \left(\frac{\partial R}{\partial x_n} \cdot u_{x_n}\right)^2} \tag{C.2.2}$$

C.3 Example Uncertainty Calculation

The following shows how the uncertainty of λ was determined and is given as an example of how all uncertainties listed in Tables 4.2 and 4.3 in Chapter 4 were calculated. This particular example was taken from Kastanis' thesis[21] and verified to match the formulas used to calculate λ for all tests presented in this paper.

The Relative Air-Fuel Ratio, λ, is calculated as

$$\lambda = \frac{\dot{m}_{air,dry}}{\dot{m}_{fuel}} \cdot \frac{1}{(A/F)_{stioch}} \tag{C.3.1}$$

where $\dot{m}_{air,dry}$is the mass flow of air entering the engine, $\dot{m}_{fuel}$is the mass flow rate of the fuel and $(A/F)_{stioch}$is the stoichiometic air fuel ratio. The mass flow rate of the fuel is given as

$$\dot{m}_{fuel} = \dot{m}_{fuel,homo} + \dot{m}_{fuel,strat} \tag{C.3.2}$$

where $\dot{m}_{fuel,homo}$is the mass flow rate of the fuel for the homogeneous, bulk charge and $\dot{m}_{fuel,strat}$is the mass flow rate of the fuel for the stratified, PSC charge including both primary and secondary injections. The the mass flow of air entering the engine is given by

$$\dot{m}_{air,dry} = \frac{1}{1+\omega} \cdot \rho_{air} \cdot \dot{V}_{air} \tag{C.3.3}$$

where $\omega$is the specific humidity, ρ_{air} is the density and $\dot{V}_{air}$ is the volumetric flow rate, of the air entering the engine. The volumetric flow rate is given by

$$\dot{V}_{air} = \left(B \cdot \triangle P_{LFE} + C \cdot \triangle P_{LFE}^2\right) \cdot \mu_{std} \cdot \frac{110.4 + T_{air}}{14.58 \cdot T_{air}^{3/2}} \tag{C.3.4}$$

where $\triangle P_{LFE}$ is the pressure drop across the LFE, B and C are constants specific to the the LFE pressure measuring device, μ_{std} is the viscosity of air at standard conditions and T_{air} is the air temperature. The air density is calculated as

$$\rho_{air} = \frac{\frac{P_{air}}{R_{air}} + P_{H_2O} \cdot \left(\frac{1}{R_{H_2O}} - \frac{1}{R_{air}}\right)}{T_{air}} \tag{C.3.5}$$

where $P_{air}$is the air pressure, $R_{air}$is the gas constant for air, $P_{H_2O}$is the partial pres-

sure of the water in the air and $R_{H_2O}$is the gas constant for water. The specific humidity is calculated as

$$\omega = 0.62198 \cdot \frac{P_{H_2O}}{P_{air} - P_{H_2O}} \tag{C.3.6}$$

and the partial pressure of the water in the air is calculated as

$$P_{H_2O} = RH \cdot P_{sat,H_2O} \tag{C.3.7}$$

where RH is the relative humidity and P_{sat,H_2O} is the saturation pressure of the water in the intake air. Based on the formulas above, λ is a function of the following measured variables

$$\lambda = \lambda\left(\triangle P_{LFE}, T_{air}, P_{air}, RH, \dot{m}_{fuel,homo}, \dot{m}_{fuel,strat\,fuel}\right) \tag{C.3.8}$$

The partial derivatives of $\lambda$with respect to these measured variables are as follows:

$$\frac{\partial \lambda}{\partial \triangle P_{LFE}} = \frac{\partial \lambda}{\partial \dot{m}_{air,dry}} \cdot \frac{\partial \dot{m}_{air,dry}}{\partial \dot{V}_{air}} \cdot \frac{\partial \dot{V}_{air}}{\partial \triangle P_{LFE}} \tag{C.3.9}$$

$$\frac{\partial \lambda}{\partial T_{air}} = \frac{\partial \lambda}{\partial \dot{m}_{air,dry}} \cdot \left(\frac{\partial \dot{m}_{air,dry}}{\partial \dot{V}_{air}} \cdot \frac{\partial \dot{V}_{air}}{\partial T_{air}} + \frac{\partial \dot{m}_{air,dry}}{\partial \rho_{air}} \cdot \frac{\partial \rho_{air}}{\partial T_{air}}\right) \tag{C.3.10}$$

$$\frac{\partial \lambda}{\partial P_{air}} = \frac{\partial \lambda}{\partial \dot{m}_{air,dry}} \cdot \left(\frac{\partial \dot{m}_{air,dry}}{\partial \rho_{air}} \cdot \frac{\partial \rho_{air}}{\partial P_{air}} + \frac{\partial \dot{m}_{air,dry}}{\partial \omega} \cdot \frac{\partial \omega}{\partial P_{air}}\right) \tag{C.3.11}$$

$$\frac{\partial \lambda}{\partial RH} = \frac{\partial \lambda}{\partial \dot{m}_{air,dry}} \cdot \left(\frac{\partial \dot{m}_{air,dry}}{\partial \rho_{air}} \cdot \frac{\partial \rho_{air}}{\partial P_{H_2O}} \cdot \frac{\partial P_{H_2O}}{\partial RH} + \frac{\partial \dot{m}_{air,dry}}{\partial \omega} \cdot \frac{\partial \omega}{\partial P_{H_2O}} \cdot \frac{\partial P_{H_2O}}{\partial RH} \right) \tag{C.3.12}$$

$$\frac{\partial \lambda}{\partial \dot{m}_{fuel,homo}} = \frac{\partial \lambda}{\partial \dot{m}_{fuel,strat}} = \frac{\dot{m}_{air,dry}}{\dot{m}_{fuel}^2} \cdot \frac{1}{(A/F)_{stioch}} \tag{C.3.13}$$

Since the partial derivatives of the measured values also contain partial derivative, these secondary partial derivatives must be calculated and are as follows:

$$\frac{\partial \dot{V}_{air}}{\partial \triangle P_{LFE}} = (B + 2 \cdot C \cdot \triangle P_{LFE}) \cdot \mu_{std} \cdot \frac{110.4 + T_{air}}{14.58 \cdot T_{air}^{3/2}} \tag{C.3.14}$$

$$\frac{\partial \dot{V}_{air}}{\partial T_{air}} = \left(B \cdot \triangle P_{LFE} + C \cdot \triangle P_{LFE}^2\right) \cdot \mu_{std} \cdot \frac{14.58 \cdot T_{air}^{3/2} - (110.4 + T_{air}) \cdot \left(\frac{3}{2} \cdot 14.58 \cdot T_{air}^{1/2}\right)}{14.58^2 \cdot T_{air}^3} \tag{C.3.15}$$

$$\frac{\partial \rho_{air}}{\partial P_{air}} = \frac{1}{R_{air} \cdot T_{air}} \tag{C.3.16}$$

$$\frac{\partial \rho_{air}}{\partial P_{H_2O}} = \frac{\frac{1}{R_{H_2O}} - \frac{1}{R_{air}}}{T_{air}} \tag{C.3.17}$$

$$\frac{\partial \rho_{air}}{\partial T_{air}} = -\frac{\frac{P_{air}}{R_{air}} + P_{H_2O} \cdot \left(\frac{1}{R_{H_2O}} - \frac{1}{R_{air}}\right)}{T_{air}^2} \tag{C.3.18}$$

$$\frac{\partial \omega}{\partial P_{air}} = -0.62198 \cdot \frac{P_{H_2O}}{(P_{air} - P_{H_2O})^2} \tag{C.3.19}$$

$$\frac{\partial \omega}{\partial P_{H_2O}} = 0.62198 \cdot \frac{P_{air}}{(P_{air} - P_{H_2O})^2} \tag{C.3.20}$$

$$\frac{\partial \dot{m}_{air,dry}}{\partial \rho_{air}} = \frac{1}{1+\omega} \cdot \dot{V}_{air} \tag{C.3.21}$$

$$\frac{\partial \dot{m}_{air,dry}}{\partial \dot{V}_{air}} = \frac{1}{1+\omega} \cdot \rho_{air} \tag{C.3.22}$$

$$\frac{\partial \dot{m}_{air,dry}}{\partial \omega} = -\frac{1}{(1+\omega)^2} \cdot \rho_{air} \cdot \dot{V}_{air} \tag{C.3.23}$$

$$\frac{\partial P_{H_2O}}{\partial RH} = P_{sat,H_2O} \tag{C.3.24}$$

$$\frac{\partial \lambda}{\partial \dot{m}_{air,dry}} = \frac{1}{\dot{m}_{fuel} \cdot (A/F)_{stoich}} \tag{C.3.25}$$

Using the formulas above, the uncertainty of λ with respect to the measured variables can be calculated as follows:

$$w_\lambda^2 = \left(\frac{\partial \lambda}{\partial \triangle P_{LFE}} \cdot w_{\triangle P_{LFE}}\right)^2 + \left(\frac{\partial \lambda}{\partial T_{air}} \cdot w_{T_{air}}\right)^2 + \left(\frac{\partial \lambda}{\partial P_{air}} \cdot w_{P_{air}}\right)^2 + \left(\frac{\partial \lambda}{\partial RH} \cdot w_{RH}\right)^2$$

$$+\left(\frac{\partial\lambda}{\partial\dot{m}_{fuel,homo}}\cdot w_{\dot{m}_{fuel,homo}}\right)^2+\left(\frac{\partial\lambda}{\partial\dot{m}_{fuel,strat}}\cdot w_{\dot{m}_{fuel,strat}}\right)^2 \tag{C.3.26}$$

Appendix D

Standard Engine Operating Procedure

The following is the start-up procedure for the Ricardo Hydro single-cylinder research engine in the UBC Alternative Fuels Laboratory. Please follow these steps carefully to avoid equipment damage or injury to personnel.

Initial checks and engine warm-up:

1. Turn on ventilation in test cell (Control Room PLC Panel, set fan to 50%).
2. Turn on emissions bench to allow sufficient warm-up (see separate procedure).
3. Check engine oil and coolant levels, and check around the engine for leaks.
4. Check that guards are on flywheel and timing belt.
5. Crank engine by hand once or twice (to ensure there has been no leak into the combustion chamber).
6. Check that there is no condensation in the exhaust (Valve should have been left open after last use, if not open it now). Ensure the drain is closed before engine start.

7. Turn on engine cooling water (open tap fully).

8. Start pressure transducer cooling pump (plug in).

9. Turn on ignition/injection driver box (test-cell – by DAQ).

10. Turn on thyristor drive unit in the test cell. (Main breaker on cell wall should be left on).

11. Turn on oil heater and water pump/heater (Oil heater button sticky, make sure it lights up).

12. Ensure that back pressure valve control box is powered and that valve is plugged in (not currently in set-up).

13. While oil and water are heating, calibrate emissions bench (see separate procedure).

14. Turn on power to transducer and channel boxes.

Starting the engine software:

1. Turn on test cell computer.

2. Open TimingControl on the desktop and press the arrow button to start the program (engine will not start sparking until the switch on the control panel is switched on).

3. Open DynoServer V7.6 DI Lift added on desktop (this program is not currently varied during engine operation but must be open in order for the computers to communicate).

4. Turn on the control room computer.

5. Open VNC. Move test cell computer screen view to left screen.

6. Open Dynoclient and select file to save data to (in D:\ drive). The file name should have the following format: <date>_<user>_<speed>_<throttle%>_<test description>.csv, for example: “031121_CR_2000rpm_100%_homogeneous_lean_limit_noPSC.csv”. (Note: If not acquiring data, open “junkdynodata.csv”.) The file must be in “csv” format or no data will be recorded.

7. Open Pressureclient.

8. Open/run Performance_NG_Runtime_(EGR_DI) and move to left screen. When hitting the get data button it will give a more accurate lambda reading.

Starting the Engine:

1. Reset emergency stop buttons (one on post by engine, one on control panel).

2. Open the two green NG valves in test cell, and the NG valve in the control room.

3. Turn on ignition switch (control panel).

4. Check oil temperature is greater than 60ºC

5. Check (control panel):

    - Speed setting is at 3.0 (1500 rpm)
    - Throttle setting is at 50%
    - Fuel setting is at 2.2

6. Make a note of the following in the Ricardo Logbook:

    - Date
    - Engine hours
    - Speed and Load
    - Operator Comment (test description) and initials

7. Press “reset” then immediately press green “start” button.

Firing the Engine: (Engine firing is always started at 1500rpm, 50% Throttle, Lambda 1.0 and MBT Spark)

1. In Timing Controller set spark timing to –23 deg, (“duration” should be set to 1.0 deg). Turn on ignition.

2. Check fuel control is set to “flow” (switch 1) then turn on (switch 2). Engine should fire. (Note that fuel flow output on DAQ should be 0.8 kg/h – this corresponds to lambda 1.0).

3. After one minute of firing, turn on AFRecorder (lambda sensor): Press “sys”, “6” (says ‘enable’), “ENT”, “1” (says ‘measure’).

4. Wait until oil temperature is approx. 90ºC and coolant temperature is approx 95ºC before beginning to acquire data.

Important Note: If testing for a long time, may need to recalibrate the emissions bench, as the calibration of the instruments drifts with changing temperature. Recommended

Practice: Before proceeding with the test, run the engine at the above "standard" conditions for at least 20 mins, and acquire data at this point (for repeatability). The emissions bench can be calibrated during this time.

Acquiring Data:

1. Set test point. Note that when running very lean, the lambda based on mass flows is more accurate than lambda from the AFRecorder, (i.e. use Ric_Emissions_Runtime by pressing "Send data to Excel" button in Dynoclient).

2. In the paper "Test Sheet", record details of test point for future reference. 36. Record Pressure data (must be done for every test point). The file name should have the following format: <date>_<test#>_<speed>_<throttle%>_<spark>_<Lambda>_<PSCdetails>_pr.csv, for example: "031121_t05_2000rpm_50%_S23 _L1.0_noPSC_pr.csv".

3. Record Performance data: In Dynoclient, update:

   - Test number
   - Spark timing
   - PSC details (if running with PSC) Then click "Log data to File" and wait (approx. 2 mins.)

4. Set next test point and repeat data acquisition.

5. When testing is finished, return the engine to the start-up settings (1500rpm, 50% throttle, lambda 1.0).

Shutting down the engine:

1. Turn off the NG supply at the flow-meter.

2. Turn off ignition (Timing Controller on computer, and ignition switch on control panel)

3. Allow engine to motor briefly, until exhaust temperature drops below 130ºC.

4. Press red “dyno” stop button. Engine will come to a complete stop.

5. Turn off oil/water heaters (but not the pumps).

6. About two minutes after firing stops, disable AFRecorder.

    - Press “sys”, “6” (says ‘enable’), “ENT”, “1” (says ‘measure’).
    - Display should now read ‘Sensor Disabled’

7. Close all three NG valves on NG lines.

8. Turn off switch on ignition/injection box in test cell.

9. When engine has cooled (after at least fifteen minutes):

    - Turn off oil and water pumps.
    - Turn off the thyristor drive breaker.
    - Turn off cooling water tap and unplug pressure transducer cooling pump.
    - Open exhaust drain valve. If valve is left closed water may back-up all the way into the cylinder before next use.
    - Shut down emissions bench.

10. Stop all software (in reverse order to starting) and shut down control room computer.

11. When testing is complete and engine shut down, stop the Dynoclient – this closes the file you have been saving performance data to. (if you wish to continue monitoring engine conditions during the cool-down stage, start Dynoclient again and use “junkdynodata.csv”).

12. Comment on any important issues in the Ricardo Logbook, record engine hours and running time.

EMERGENCY SHUT DOWN: Hit red “STOP” button in Test cell or on Control Panel. Ignition and dyno are disabled and the engine will come to a complete stop.

Note that fuel does not shut off automatically, nor are there gas detectors in the cell connected to the ESD. (These issues are addressed in the new CERC cells).

Do not use the emergency stop button unless necessary.

Appendix E

Minimum Advance for Best Torque Technique

The Minimum Advance for Best Torque (MBT)[4] technique is a means of finding the spark timing that gives optimum engine performance. The definition of optimum engine performance, in this case, is the conditions where the engine produces the greatest torque. This happens when the spark timing is more advanced with respect to the top dead center (TDC) engine position between the compression and power strokes. Advancing the timing too much will cause rapid combustion of the air-fuel mixture creating very high cylinder pressures. Too avoid advancing the timing too far a test is run over a range of spark timings.

The spark timing is advanced significantly more than what is estimated to be the MBT timing. The spark timing is then slowly reduced bringing the timing closer to TDC. The torque is recorded and plotted for each spark timing tested and a graph similar to that presented below is created.

The point labeled on the graph is the MBT spark timing. It is the point where the

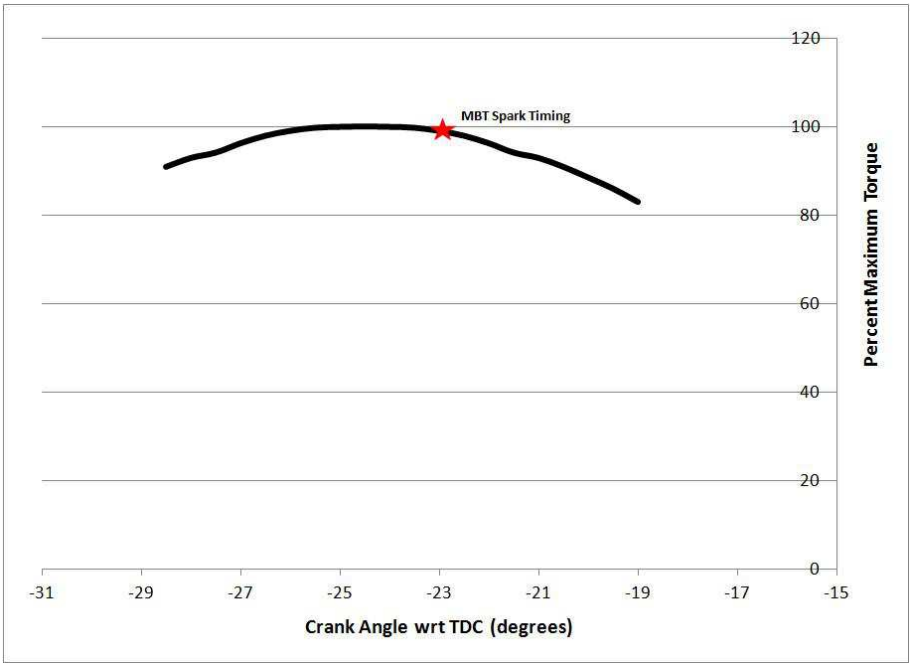

Figure E.1: MBT Spark Timing Graph

engine torque begins to rapidly decrease with less advanced spark timing.

This method was used for determine the spark timing used in all test presented in this paper. It can be seen that the point chosen as MBT is not well defined. Also, when running the engine at high λ values the stability of this curve decreases. To help reduce the error in determining the MBT timing, the test was performed 3 times for each data point and the same spark timing was used for all single and double-PSC-injection test at a given λ and engine speed.